ELSEVIER

Journal of African Earth Sciences 39 (2004) 25–62

Journal of African Earth Sciences

www.elsevier.com/locate/jafrearsci

Paleogene and Cretaceous sediment cores from the Kilwa and Lindi areas of coastal Tanzania: Tanzania Drilling Project Sites 1–5

Paul N. Pearson [a,*], Christopher J. Nicholas [b], Joyce M. Singano [c], Paul R. Bown [d], Helen K. Coxall [e], Bart E. van Dongen [f], Brian T. Huber [g], Amina Karega [c], Jackie A. Lees [d], Emma Msaky [c], Richard D. Pancost [f], Marion Pearson [b], Andrew P. Roberts [e]

[a] *School of Earth, Ocean and Planetary Sciences, Cardiff University, Main Building, Park Place, Cardiff CF10 3YE, UK*
[b] *Department of Geology, Trinity College, Dublin 2, Ireland*
[c] *Tanzania Petroleum Development Corporation, P.O. Box 2774, Dar-es-Salaam, Tanzania*
[d] *Department of Earth Sciences, University College London, Gower Street, London WC1E 6BT, UK*
[e] *School of Ocean and Earth Science, University of Southampton, Southampton Oceanography Centre, European Way, Southampton SO14 3ZH, UK*
[f] *Organic Geochemistry Unit, Biogeochemistry Research Centre, School of Chemistry, Cantock's Close, Bristol University, Bristol BS8 1TS, UK*
[g] *Department of Paleobiology, MRC NHB-121, P.O. Box 37012, Smithsonian National Museum of Natural History, 10th and Constitution Avenue, Washington, DC 20012-7012, USA*

Received 18 September 2003; accepted 3 May 2004
Available online 28 July 2004

Abstract

Initial results of scientific drilling in southern coastal Tanzania are described. A total of five sites was drilled (mostly using continuous coring) by the Tanzania Drilling Project for paleoclimate studies. The sediments are predominantly clays and claystones deposited in a deep marine shelf environment and often contain excellently preserved microfossils suitable for geochemical analysis. The studies reported here include summaries of the lithostratigraphy, biostratigraphy (planktonic foraminifers, calcareous nannofossils, benthic foraminifers, and palynology), magnetostratigraphy, and organic geochemistry.

TDP Site 1 was drilled near Kilwa Masoko airstrip (8°54.516′S, 39°30.397′E). It yielded 8.55 m of barren blue-grey clays that may be Miocene in age, followed by 1.2 m of greenish-black to dark greenish-grey clay probably of the same age. The remainder of the hole cored 62.35 m of lower Oligocene sediments (nannofossil Zone NP23), which are predominantly greenish-black to dark greenish-grey clays. Total penetration was 74.10 m. The coring represents the first report of a thick Oligocene clay formation in the area.

TDP Site 2 was drilled near Kilwa Masoko prison (8°55.277′S, 39°30.219′E). It yielded 92.78 m of predominantly dark greenish-grey clay with occasional allochthonous limestone beds that consist mostly of redeposited larger foraminifers. The site encompasses lower to middle Eocene planktonic foraminifer Zones P8/9 to P11 and nannofossil Subzones NP14b to NP15c. It encompasses a rarely cored interval across the Ypresian–Lutetian transition.

TDP Site 3 was drilled near Mpara in the Kilwa area (8°51.585′S, 39°27.655′E). It yielded 56.4 m of predominantly dark greenish-grey clays and claystones. The site is assigned to lower Eocene planktonic foraminifer Zone P6 and nannofossil Zone NP11.

TDP Site 4 was drilled near Ras Tipuli on the northwest side of Lindi creek (9°56.999′S, 39°42.985′E). It yielded 19.8 m of predominantly dark greenish-grey clay with allochthonous limestone interbeds. The site encompasses middle Eocene planktonic foraminifer Zones P12–P14 and nannofossil Zone NP17.

TDP Site 5 was drilled at Machole, near Lindi, south of Kitulo Hill (10°01.646′S, 39°41.375′E). It yielded 31.6 m of predominantly greenish-black to dark greenish-grey clay assigned to the upper Cretaceous *Globotruncana falsostuarti* planktonic foraminifer zone and nannofossil zones UC15e–UC17 (upper Campanian–lower Maastrichtian). Paleomagnetic analysis suggests that the site straddles two magnetic reversals, between Chrons C32r.2r and C32r.1n.

Samples from TDP Sites 1–5 yielded dinocyst and miospore assemblages that are integrated with the calcareous stratigraphy. Organic geochemical analyses of samples from each of the cores revealed biomarkers of predominantly terrestrial origin and an

* Corresponding author.
E-mail address: pearsonp@cardiff.ac.uk (P.N. Pearson).

0899-5362/$ - see front matter
doi:10.1016/j.jafrearsci.2004.05.001

unusually low degree of thermal maturity, suggesting shallow burial depths. X-ray diffraction studies suggest that much of the Paleogene clay may be reworked from eroded Mesozoic formations.

Keywords: Cretaceous; Eocene; Oligocene; Foraminifers; Nannofossils; Geochemistry; Palynology; Magnetostratigraphy

1. Introduction

Cretaceous marine sediments crop out along most of the Tanzanian coastal region south of Dar-es-Salaam (Kent et al., 1971). The overlying Paleogene deposits are less widespread and occur in several large outliers further north and on the island of Pemba. However, the most extensive outcrop is a continuous strip along the coast in the south of the country, between the administrative centres of Kilwa and Lindi (Kent et al., 1971; Schlüter, 1997, Fig. 1). The predominant lithology of both the Cretaceous and Paleogene sediments is clay or claystone, often punctuated by thin carbonate or siliciclastic turbidites, although thicker sand bodies and reefal limestones also occur in parts of the Lower Cretaceous and Paleocene succession respectively (see Kent et al., 1971). In this paper we describe the initial results of recent scientific coring in this area, including the lithostratigraphy, biostratigraphy (based on planktonic and benthic foraminifers, nannofossils, and palynomorphs), organic geochemistry, and magnetostratigraphy of five new drill sites. This work is the first detailed synthetic study of these sediments and will provide the framework for further geochemical and paleoceanographic research on the cores. It will also help define the litho- and sequence-stratigraphy of this part of the East African passive margin.

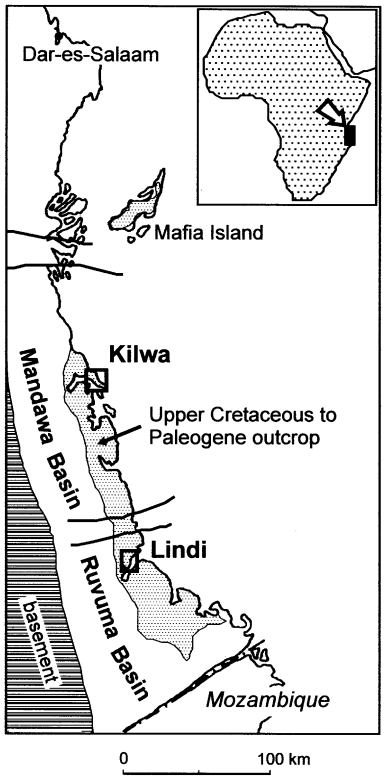

Fig. 1. Map of the study areas in relation to the Upper Cretaceous and Paleogene outcrop in southern Tanzania. Areas of detailed investigation around Kilwa and Lindi are highlighted.

The presence of Paleogene and Cretaceous sediments in southern coastal Tanzania has been recognized since the late 19th century (see Haughton, 1938 and Kent et al., 1971 for a review). The area became internationally prominent with the publication of Blow and Banner's (1962) detailed micropaleontological and biostratigraphic work in the area. Blow and Banner (1962) and Blow (1979) used excellently preserved material collected by BP-Shell exploration geologists (R. Stoneley and F.C.R. Martin) in the 1950s to name many new species of planktonic foraminifers that are now widely used for global stratigraphic correlation, and they also typified several foraminifer biozones in the upper Eocene and lower Oligocene of the Lindi area that continue to be used internationally. Additional information on the microfossils of the area was presented by Bate and Bayliss (1969), Fahrion (1937), and Ahmad et al. (1991).

We were initially drawn to the area because of the excellent preservation of the planktonic foraminifer shells. These commonly appear glassy and reflective under the light microscope, and with the scanning electron microscope they show smooth surfaces and the original microgranular textures on a micron scale. The reason for the excellent preservation appears to be that the shells are mostly encased in clay, which being impermeable, hinders recrystallization in the presence of migrating fluids. Also, the sediments in this area were never deeply buried (as confirmed by their extreme thermal immaturity; see below). In recent years, there has been a growing appreciation among geochemists that such material, although rare, is valuable for paleoclimate studies. This is because the more common carbonate chalks and oozes of the deep ocean tend to be recrystallized, affecting the geochemistry and isotope ratios of the shells (Norris and Wilson, 1998; Pearson et al., 2001, 2002; Wilson and Norris, 2001; Wilson et al., 2002; Norris et al., 2002).

The current phase of investigation began in 1998 in a project funded by Britain's Natural Environment Research Council (NERC) in collaboration with the Tanzania Petroleum Development Corporation

(TPDC). The initial aim was to collect foraminifer samples from outcrops in order to conduct oxygen isotope analysis and thereby to determine ancient tropical sea surface temperatures in the region. Field expeditions in 1998, 1999, and 2000 resulted in the collection of about 500 outcrop samples from the areas around and between Kilwa and Lindi. Many of these samples produced biostratigraphic age determinations, allowing us to refine the outcrop patterns of Cretaceous and Paleogene units in the area. Our field observations have also begun to yield a new understanding of the tectonics and structural geology of the area (see Section 2 below). Initial geochemical results from selected outcrop samples were presented by Pearson et al. (2001).

Following this phase of investigation, additional funds were obtained from NERC to support shallow drilling of the Cretaceous and Paleogene sediments. The principal aim of the drilling was to obtain suitable samples for both boron isotope analysis of foraminifer shells and carbon isotope analysis of biomarkers to estimate ancient levels of atmospheric carbon dioxide. The material obtained is, in addition, useful for a wide range of micropaleontological, stratigraphic and paleoceanographic purposes. A broad team was assembled from the United Kingdom, Tanzania, Ireland and the United States to collaborate on this work, as the Tanzania Drilling Project (TDP). Here we describe the initial results from the first year of drilling that took place in 2002.

2. Geological overview

2.1. Tectonic history

The geology of the area is strongly affected by the two-stage break-up of Gondwana, which began at about 300 Ma (Salman and Abdula, 1995). An initial rifting phase from 300 to 205 Ma created extended rift systems across the continent which filled with thick siliciclastic and carbonate sediments of the Karoo Group. The second phase from about 205 to 157 Ma marked the actual fragmentation of Gondwana, and was accompanied by the extrusion of extensive flood basalts. From about 157 Ma, active sea-floor spreading in the Western Somalia and Mozambique Channel Basins separated Gondwana into West (Africa and South America) and East (Antarctica, India and Sri Lanka, Madagascar, Seychelles and Australia) blocks, with the divergence of the two concentrated along the major transform zones of the Davie Ridge, Mozambique Escarpment and Explora Escarpment in Antarctica (Lawver et al., 1992; Salman and Abdula, 1995). This rifting and spreading was accompanied by a major marine transgression onto the passive continental margins of both West and East Gondwanan blocks. In Tanzania, this resulted in thick Upper Jurassic and Lower Cretaceous sedimentation in a series of marginal basins, which include the Mandawa and Ruvuma Basins of the study area (see Fig. 1).

By the end of the Early Cretaceous, the axis of spreading had jumped east of Madagascar which resulted in a period of stabilization along the East African margin. A Late Cretaceous transgression resulted in widespread deepwater clay and mud facies accumulating in offshore basins, and similar conditions continued into the Paleogene. Thick clay deposits are particularly well developed along coastal Tanzania. Although sedimentation was probably rather episodic, almost every planktonic foraminifer zone of the Late Cretaceous and Paleogene has been recorded on the Tanzanian shelf (Blow, 1979).

By about 35 Ma the current East African Rift system had been initiated. This was followed by renewed tectonic movement along the Davie and Mozambique submarine ridges (Salman and Abdula, 1995). A mantle plume with a head diameter of about 600 km may currently exist beneath the East African plateau and Tanzania. Two arms from this plume appear to penetrate the lithosphere at a shallow level below the East and West arms of the African Rift System (Simiyu and Keller, 1997).

Our drilling has concentrated upon the thick passive margin sequences developed in the Mandawa (Kilwa area) and Ruvuma (Lindi area) Basins during the 'stabilization' phase after Gondwana's break-up. However, it is now emerging from our field work and from the TDP drilling that these basins have remained tectonically active until relatively recently. For instance, TPDC onshore seismic lines demonstrate 'pop-up' flower structures with reactivated normal faults. This compressional reactivation has occurred since the Miocene. It is still not clear whether this later tectonic activity is due to movement along the Davie Ridge, plume activity or a combination of both these factors.

2.2. The Kilwa area

The principal fieldwork conducted in the Kilwa area prior to this study was by Hennig (1937) and R. Stoneley in the 1950s, with more recent observations on the Cretaceous by Gierlowski-Kordesch and Ernst (1987) and Ernst and Zander (1993). Stoneley's informal stratigraphy and maps were subsequently summarized and published by the Geological Survey of Tanzania as the '1:125 000 Sheet 256 Kilwa' (Moore et al., 1963). This has remained the most detailed published geological summary of the area. Exposure today is poor and concentrated around the shoreline and roadside cuttings.

Stoneley subdivided the Paleogene of the Kilwa Masoko peninsula into two broad, unnamed units representing the Paleocene and the Middle Eocene (Moore

et al., 1963). Two possible Miocene outcrops were also identified in Kilwa Creek, but these have now been obscured by mangrove swamp. Reconnaissance field surveying in 1998, 1999 and 2000 resulted in the collection of about 300 sediment and soil samples from the area, many of which have subsequently yielded accurate age determinations based on their planktonic foraminifer biostratigraphy. This has aided TDP site selection, although it has now become clear that there are several post-Miocene faults in the area that are not shown on the Geological Survey map. A new structural survey is currently underway. The Paleogene in TDP Sites 1, 2 and 3, allied with the field data, naturally divides into three major units. These are Oligocene (to possibly Miocene) greenish black clays, Lower to Middle Eocene (P6a–P11) dark greenish-grey clays and claystones, and Paleocene clays with reef limestones.

The Cretaceous sediments of the Kilwa area have yet to be drilled by the TDP, but were studied in outcrop by Ernst and Zander (1993). Schlüter (1997) named the Kilwa Group for these Upper Cretaceous sediments but he did not divide them into Formations. Apart from this, no formal stratigraphic nomenclature exists for the area.

2.3. The Lindi area

Previous early work in the Lindi area informally established lithostratigraphic units for the Eocene (see Haughton, 1938, for review). The Lukuledi Beds south of Lindi Creek were composed of two units, the Miocene 'Lindi Uppermost Beds' and below these, the Paleogene 'Kitunda Beds'. North-west of the Creek, other Paleogene deposits named the 'Kitulo Beds' were recognized in and around the town of Lindi and on the flanks of neighbouring Kitulo Hill.

The BP-Shell geologist F.C.R. Martin surveyed the area in the 1950s, but the only published maps for the area are those in Blow and Banner (1962) and Kent et al. (1971), which are based on Martin's field map. Our own field reconnaissance in the Lindi area has shown it to have much better exposure than Kilwa. Field samples from previous years have established that Upper Cretaceous to Middle Eocene clay units are exposed around the coast from south-west of Kitulo Hill to Ras Tipuli in the north of Lindi Creek. Upper Eocene clays are exposed to the north and inland from Ras Tipuli.

As at Kilwa, relatively recent compressional tectonics have affected the Lindi area. Fault zones can be observed in the field and appear to be reactivated and reversed normal faults. Thrust structures are present at Ras Mtama and Ras Tipuli on the coast north of Lindi. Added to this structural complication is the inherent incompetence of the thick clay units which causes local slope failure. Further surface mapping and drilling by the TDP will result in a new geological map for the Lindi area.

3. Methods

3.1. Drilling operations

Five sites were drilled in September–October 2002, three in the vicinity of Kilwa (TDP Sites 1–3) and two near Lindi (TDP Sites 4 and 5). Sites were selected to obtain a widespread of sediment ages in the best preserved microfossil material possible. In general, drill sites were located near outcrops that have previously yielded well-preserved foraminifers.

Sites were cored using a truck-mounted rig (Fig. 2), with a core diameter of 2 in. ($\sim$5 cm) and typical core lengths of 3 m, using water and mud circulation to avoid unnecessary organic contamination. A scientific team was on site during drilling to describe and sample the cores. Drilling operations were considerably slowed by failure of the wireline coring system on the rig, which necessitated removal of the entire drill string for each core obtained. This limited the practical depth of penetration to about 100 m. Nevertheless, this allowed us to obtain samples from below the zone of surface oxidation and contamination by modern terrestrial organic matter, which was our primary aim.

After recovery, each core was laid on an aluminium sheet and cleaned of adhering drilling mud. Cores were photographed and the lithologies described. Some samples for planktonic foraminifer biostratigraphy were studied on site. Further samples were dispersed to various laboratories for further study of the foraminifers, and additional work on the calcareous nannofossil biostratigraphy, palynology, paleomagnetics, organic geochemistry and lithostratigraphy. After sampling, cores were cut into sections of 1 m length, wrapped in polythene and transferred to wooden core-boxes. All cores are archived at TPDC in Dar-es-Salaam. Requests for core samples, photographs or Visual Core Description (VCD) sheets should be directed to the corresponding author.

Sample identification numbers are modelled on the procedure used by the Ocean Drilling Program. Tables showing the depth of each core obtained are given in the relevant sections below. A typical sample identifier refers to the site, core number, section number, and depth in cm from the top of that section. For example, Sample TDP2/27-2, 16–20 cm was taken from Tanzania Drilling Project Site 2, Core 27, Section 2, between 16 and 20 cm from the top of that 1 m section. The depth of this sample can be calculated by adding 1 m for Section 1, plus 16–20 cm to the depth from the top of the core (66.70 m + 1.16 m = 67.86 m). The following code refers to the purpose of the samples; B = benthic (larger)

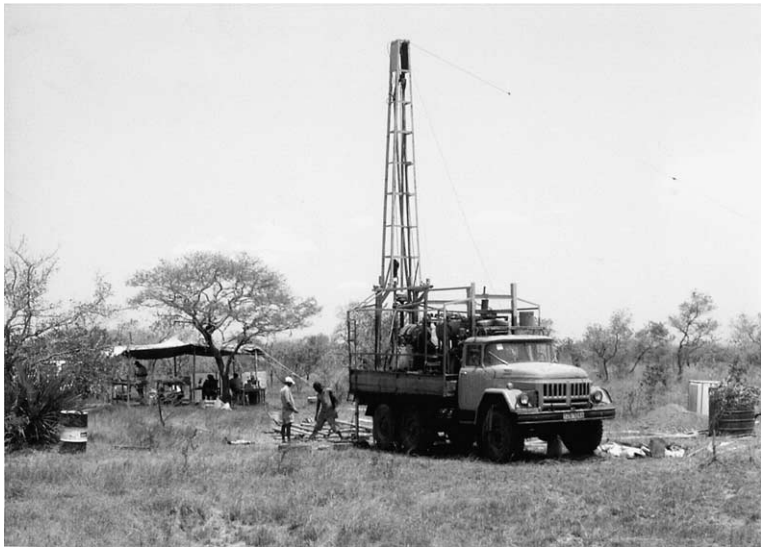

Fig. 2. Photograph of drilling operations at TDP Site 3, showing the truck-mounted rig and mobile field laboratory (background).

foraminifers, L = lithostratigraphy, F = foraminifers, M = paleomagnetic analysis, N = nannoplankton, O = organic chemistry, T = TPDC palynology and smaller benthic foraminifers.

3.2. Lithostratigraphy

All lithological descriptions were undertaken on site immediately after core recovery. Cores were removed from the core barrel and laid out on cleaned corrugated aluminium sheets. These were placed on description tables and sprayed down with water to remove as much of the drilling mud as possible. Where this mud adhered to the cores they were shaved using a metal peeler, which removed the contaminant coating and exposed the internal clay for description. All cores were cut into 1 m sections and photographed before description. Because most of the cores contain fresh, soft clay, photography and visual description were made as quickly as possible to avoid problems of desiccation, shrinkage and subsequent fragmentation.

Ocean Drilling Programme style Visual Core Description (VCD) sheets were used to record information in a series of columns. In addition, to help with consistency, ODP terminology for sediment description was also followed as closely as possible. Observations were made on the principal lithology in the core, followed by any comments regarding any subsidiary or secondary lithologies present. Colour variation was described using the Geological Society of America rock colour chart (based on Munsell Soil colours). All sedimentary structures were noted and finally the presence of drilling disturbance was recorded. Unusual lithologies such as limestone beds were sampled and thin sections prepared. Lithologies were described in the field by Nicholas and Roberts.

For X-ray diffraction (XRD) analysis, which were conducted by M. Pearson at Trinity College, Dublin, samples were reduced to a fine powder. 5 g of powder was placed in a 100 ml radiated cylinder and a small amount of dispersing solution added. The remainder of the cylinder was then filled up to 100 ml with de-ionized water. The tube was shaken vigorously and left overnight. After this, the tube was shaken vigorously again and left to settle for exactly 3 h. A pipette dipped into the solution to a depth of exactly 3.9 cm removed a clay fraction of less than 2μ. Samples were pipetted onto wafers and air dried. The X-ray generator was a Phillips PW1720 with a Phillips PW1050/25 diffractometer and a Phillips PW3313/20 Cu Kα anode tube that was run with standard conditions of 40 kV and 20 mA. A soller slit and a 1° divergence slit were used on the incident X-ray beam and a anti-scatter slit followed by a 0.25° receiving slit were used on the diffracted beam, in front of the AMR detector. The detector controller was a Hilton Brooks. All measurements were taken from 5 to 40° (2θ) at a step size of 0.02 degree per second. Sample wafers were analysed twice. After the first trace had been acquired, wafers were glycolated overnight at 60 °C. Swelling clays such as the smectite group reduce their 2θ angle following glycolation and thus produce peak shifts when re-analysed.

Carbon, hydrogen and nitrogen abundances were determined on a Carlo Erba EA 1108 by van Dongen at Bristol University. The amounts of sulfur and carbon present as carbonate were determined on a Coulomat 702 (Strohlein). The total organic carbon contents (TOC) were determined by subtracting the amounts of

carbon present as carbonate from the total carbon content. All values reported are averages of duplicate measurements and have an error of ±0.2%.

3.3. Planktonic foraminifers

Clay samples were placed in beakers and gently disaggregated by hand in tap-water. The clay was then washed over sieves, generally using 63 and 250 μm meshes. Residues were transferred to filter paper and dried in the sun or in an oven at 40 °C before being placed in sample jars. Sample preservation was qualitatively assigned to the following categories: Excellent (E), Good (G), Moderate (M), Poor (P), and Barren (B). The reason for poor preservation was generally overgrowth and infilling of shells by secondary calcite, or pyritisation. The presence of calcite infillings and extensive pyrite was documented whenever it occurred.

The full assemblage of planktonic foraminifers was recorded to species level. Planktonic foraminifer taxa were qualitatively assigned to the following abundance categories: abundant (A), common (C), rare (R) and single (S). Selected foraminifers were picked and studied using the scanning electron microscope (SEM) at Cardiff University for taxonomic purposes and to assess the state of preservation on a micron scale. These were immersed in an ultrasonic bath for 10 s to remove adhering particulates.

Samples from TDP Sites 1–4 were studied by P. Pearson and Coxall at Cardiff University, UK. Samples from TDP Site 5 were studied by Huber at the US National Museum. Planktonic foraminifer biozones were identified using the standard tropical zonation schemes of Berggren et al. (1995) and Gradstein et al. (1995). Full species-level range-charts were constructed and will be published elsewhere.

3.4. Calcareous nannofossils

Samples were prepared as smear-slides (Bown and Young, 1998) and analysed using a Zeiss Axiophot transmitting light microscope at 1000× magnification (for the Paleogene) and an Olympus BH-2 transmitting light microscope at 1250× magnification (for the Cretaceous) in cross-polarized and phase-contrast light. Assemblages were logged semi-quantitatively, and slides were observed for at least 30 min, in most cases much longer. Digital images were captured using a Zeiss Axiophot microscope with video attachment and NIH Image Freeware. Nannofossil abundance to background sediment was estimated as M = moderate (approximately equal particulate proportions) to H = high (with more nannofossil particles than sediment). Abundance categories used are A = abundant (>10 specimens per field of view); C = common (1–10 specimens per field of view); F = frequent (1 specimen per field of view); R = rare (<1 specimen per field of view). Preservation was assessed as G = good (no etching or overgrowth); M = moderate (some etching or overgrowth); or P = poor (significant etching or overgrowth). The work was conducted by Bown and Lees at University College London (UCL). Sample material, slides and images are archived in the micropaleontology unit at UCL.

For the Paleogene, the biozones of Martini (1971) were used, along with the additional middle Eocene subzones of Aubry (1991). The alternative bioevents used in the Okada and Bukry (1980) biozonation were also considered, where appropriate. The time-scale calibration used is that of Lyle et al. (2002). For the upper Cretaceous, the zones of Burnett (1998) were used, as well as those of Sissingh (1977), as modified by Perch-Nielsen (1985).

3.5. Benthic foraminifers

Sample preparation was as for planktonic foraminifers. Because species diversity is much higher than for planktonic foraminifers, and the samples contain many undescribed species, most identification was to genus level. Benthic foraminifers were studied by Karega and Singano at TPDC, and SEM work was done by Karega at Cardiff University. Ratios of Planktonic to Benthic foraminifers (P:B ratios) in the coarse fraction (>250 μm) were counted in selected samples by spreading the samples evenly on a picking tray and counting the first 300 specimens, or fewer if there were less specimens. Benthic foraminifers were assigned to the same abundance and preservation categories as planktonic foraminifers.

3.6. Palynology

The palynological preparation technique was as described in Barss and Williams (1973). Palynomorphs were extracted from about 10 g of sediment. Hydrochloric acid and hydrofluoric acid treatments were used to remove carbonates and silicates, carefully followed by decantation and neutralization of residues. A residue bottle was filled with the samples halfway, and an equal amount of polyvinyl alcohol (dispersant agent) was added to the residue bottle then shaken well. Permanent slides were made (from a mixture of residue and polyvinyl alcohol). Petropaxy 154 was used as a mounting medium. Samples were studied and photographed using a Leitz-dialux 22, transmitted light microscope at 400× magnification.

Samples were studied by Msaky at TPDC, Tanzania. A complete set of samples, palynological slides and remaining residues are available in the Biostratigraphy Unit at TPDC. Dinocyst taxonomy and stratigraphic ages are from Lentin and Williams (1993).

3.7. Paleomagnetic analysis

Where possible, samples were taken for paleomagnetic analysis at intervals of between 0.5 and 1.0 m throughout the TDP cores, although only relatively undisturbed intervals were sampled. The recovered sediment is in many places strongly affected by drilling-induced deformation, where rotation of the sediment has broken the core into drilling biscuits. The thickness of the drilling biscuits is variable, and, for biscuits with thicknesses greater than a few cm, the internal structure of the sediment generally appears to be relatively unaffected by drilling, as indicated by the preservation of bedding or laminations where the lithology is not massive. Only non-biscuited core intervals, or clearly intact biscuits, were sampled for paleomagnetic analysis.

Paleomagnetic samples were taken by carving a cubic pedestal into the core using a stainless steel knife and then by placing a plastic cube (6 cm^3) over the pedestal. The samples were removed from the core by cutting the base of the pedestal with a knife. The removed samples were trimmed and plastic lids were placed onto the cubes. The up-core direction and sample name were marked on all samples. The remains of the pedestal were mostly retained for nannofossil analysis.

The cores were not azimuthally-oriented, so measured paleomagnetic declinations are meaningless. Retrieval of geomagnetic polarity for such cores is therefore entirely dependent on determining the paleomagnetic inclination. The expected present-day latitude (λ) of the drill sites (9–10°S) means that the expected inclination (I_{exp}) will be ±17.5–20°, following $\tan I_{exp} = 2\tan\lambda$. A step of 35–40° in paleomagnetic inclination would therefore be expected at any given polarity transition, which should be easily detected despite the relatively low latitude of the drill sites. Additionally, the African Plate would have been situated at a more southerly paleolatitude during the Paleogene and Cretaceous (Besse and Courtillot, 2002), which should further help to unambiguously determine the polarity of the recovered TDP cores.

The TDP paleomagnetic samples were analysed by Roberts in the paleomagnetic laboratory at the Southampton Oceanography Centre. Measurements were made using a 2-G Enterprises narrow-access, high-resolution cryogenic magnetometer that is housed within a magnetically-shielded laboratory (nominal sensitivity of the magnetometer is $\sim 10^{-6}$A/m). The magnetometer system is configured with three mutually-perpendicular in-line alternating field (AF) demagnetization coils. The samples were all stepwise AF demagnetized at applied fields of 5, 10, 15, 20, 25, 30, 35, 40, 50 and 60 mT. Additional measurements were also made for some samples after AF demagnetization at fields of 80 and 100 mT. Vector component diagrams were inspected for all samples, and, where a linear characteristic remanent magnetization (ChRM) could be identified, paleomagnetic directions were determined by performing principal component analysis on a minimum of four data points, following the method of Kirschvink (1980). For all samples, the maximum angular deviation for the identified ChRM was less than 10°.

3.8. Organic geochemistry

Samples from a range of depths at each of the sites were freeze- dried and crushed. Seven samples were chosen for biomarker analyses according to the scheme depicted in Fig. 3.

The rock powders were extracted via a Soxhlet apparatus with dichloromethane/methanol (DCM/MeOH, 2:1, v/v) for 24 h, and the total lipid extracts (TLE) were concentrated using rotary evaporation. An aliquot of the TLE was treated with activated (2 N HCl) cupper curls to remove elemental sulfur, and a mixture of three standards (androstane, hexadecane-2-ol and hexadecy-1-octadecanoate) was added. Subsequently, the aliquot was either directly derivatized as described below or separated into three fractions using bond-elute column chromatography (Strata NH_2; 5 μm, 70 A; Kim and Salem, 1990) and elution with DCM/isopropanol (2:1 v/v; 12 ml; 'neutral lipid fraction'), an acetic acid solution (a 2% solution in diethyl ether; 12 ml; 'acid fraction') and MeOH (12 ml; 'phospholipid fraction'). Further analyses were only performed on the neutral lipid and acid fractions. The neutral lipid fraction was further separated into three fractions using a column packed with (activated) alumina by elution with hexane (3 ml; 'saturated hydrocarbon fraction'), hexane/DCM (9:1 v/v; 3 ml; 'aromatic hydrocarbon fraction') and DCM/MeOH (1:1 v/v; 3 ml; 'polar fraction'). The TLE, acid and polar fractions were derivatized with BF_3 in MeOH to convert acids into their corresponding methyl esters. Subsequently, very polar compounds were removed by column chromatography over silica gel with

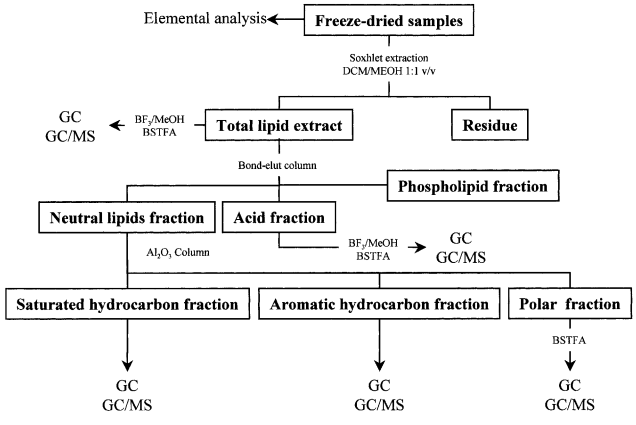

Fig. 3. Extraction and isolation scheme for organic geochemistry.

ethyl acetate as eluent. This fraction was dissolved in pyridine with bis(trimethylsilyl)trifluoroacetamide (BSTFA), and heated (70 °C; 60 min) to convert alcohols into their corresponding trimethylsilyl ethers. Gas chromatography (GC) was performed using a Hewlett Packard 5890 instrument, equipped with an on-column injector. A fused silica capillary column (50 m × 0.32 mm) coated with CP-Sil-5 (film thickness 0.12 μm), was used with hydrogen as carrier gas and the effluent was monitored by a flame-ionisation detector. The samples were injected at 50 °C and the oven was programmed to 20 °C/min at 130 °C and then at 4 °C/min to 300 °C, at which it was held isothermal for 20 min.

Gas chromatography/mass spectrometry (GC/MS) was performed using a Thermoquest Finnigan TRACE GC, equipped with an on-column injector and helium as the carrier gas, interfaced to a Thermoquest Finnigan TRACE MS, operated with electron ionisation at 70 eV and scanning a mass range of m/z 50–650 using a cycle time of 1.7 scan s^{-1}. The interface was set to 300 °C with the ion source at 240 °C. The column and temperature program were the same as described for the GC above, except helium was used as the carrier gas. Compounds were identified by comparison of mass spectra and retention time with those reported in the literature. Analyses were conducted in the Organic Geochemistry Unit at Bristol University, by van Dongen and Pancost.

Table 1 summarizes the relative abundance of biomarker classes found in the analyzed core samples. Further results are discussed in the appropriate sections below. Structures of the important biomarkers are shown in Fig. 4.

4. TDP Site 1: Kilwa Masoko 1

4.1. Site selection

TDP Site 1 was drilled in a field adjacent to the Nangurukuru road about 3 km north of Kilwa Masoko at 8°54.516′S, 39°30.397′E (Fig. 5). The Paleogene generally has a very gentle offshore dip throughout the Kilwa and Lindi areas (Kent et al., 1971). Middle Eocene strata that contain planktonic foraminifers with excellent preservation are known to be exposed in the vicinity of Kilwa Masoko prison (see Section 5 below). This site was situated slightly down-dip from the prison (where TDP Site 2 was later drilled), about 1.2 km to the north, in order to potentially drill overlying upper Eocene units. In the event, the site was found to consist mostly of Lower Oligocene clays, implying the existence of a substantial fault between TDP Site 1 and the prison. Coring was terminated when it became clear that we were drilling through a thick Oligocene formation, and although the foraminifers are very well preserved, planktonic species are scarce due to the relatively shallow water depositional environment. Table 2 shows the depths of each core and the intervals drilled and cored. An integrated summary of the lithostratigraphy and biostratigraphy for the site is shown in Fig. 6.

4.2. Lithostratigraphy

Drilling commenced on unconsolidated, well sorted and rounded, moderate yellowish brown, medium quartz sands. This sand is characteristic of the wide-

Table 1
Relative abundance[a] of biomarker classes found in the analysed core samples

Compound classes	TDP						
	1/11-1	1/20-2	2/10-3	2/25-2	3/16-2	4/1-2	5/9-3
n-Alkanes	++	++	++	++	++	++	++
n-Alkanoic acids	++	++	++	n.d.	n.d.	++	++
n-Alkanones	++	++	–	–	–	–	–
n-Alkanols	++	++	++	++	++	++	++
Archaeol	+	+	+	+	–	–	–
C_{15}/C_{15} diether	+	+	+	+	–	–	–
α-Hydroxy alkanoic acids	–	–	+	n.d.	n.d.	–	±
ω-Hydroxy alkanoic acids	++	+	++	n.d.	n.d.	+	++
Hopanes	+	+	+	+	+	+	+
Hopanoic acids	+	+	+	n.d.	n.d.	+	+
Hopanoids	+	+	+	+	+	+	+
Hopenes	+	+	+	++	+	+	+
PAHs[b]	–	++	–	–	–	–	–
Steranes	+	+	+	+	+	+	+
Steroids	+	+	±	±	+	±	+
Triterpenoids	+	++	±	+	++	+	+
Triterpenoic acids	–	+	±	n.d.	n.d.	±	–

[a] (++) abundant, (+) present, (±) trace, (–) absent, (n.d.) not determined.
[b] Polycyclic aromatic hydrocarbon.

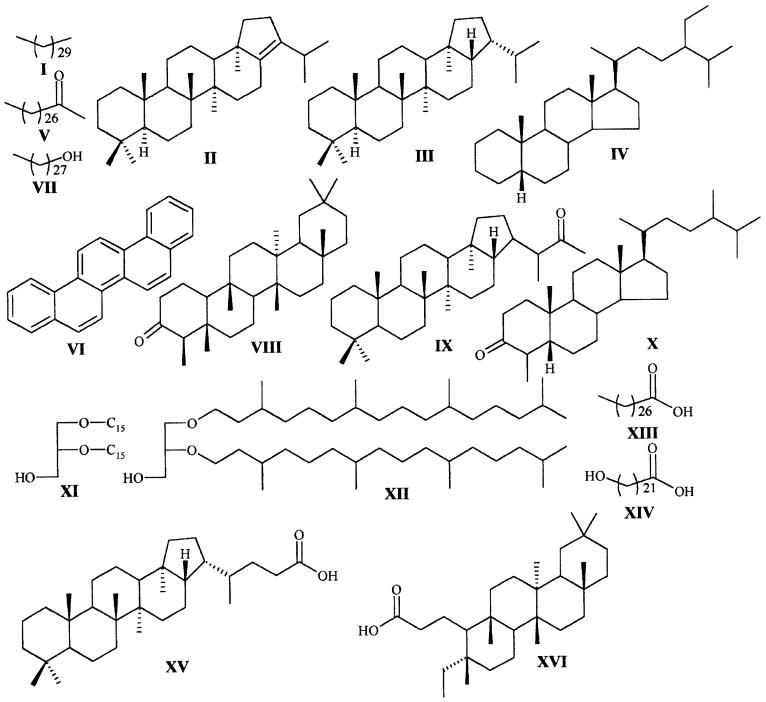

Fig. 4. Structural formulae of the principal biomarkers recorded in this study: (I) C_{31} *n*-alkane, (II) C_{30} hop-17(21)-ene, (III) 17β(H), 21β homohopane, (IV) ethylcholestane, (V) picene, (VI) C_{29} *n*-alkanone, (VII) C_{28} *n*-alkanol, (VIII) friedelan-3-one, (IX) homohopane-29-one, (X) 4,24-dimethylcholestan-3-one, (XI) glycerol dipentadecyl diether, (XII) archaeol, (XIII) C_{28} *n*-alkanoic acid, (XIV) C_{22} ω-hydroxy alkanoic acid, (XV) 17β (H), 21β (H), bishomohopanoic acid and (XVI) 3,4-seco-friedelan-3-oic acid.

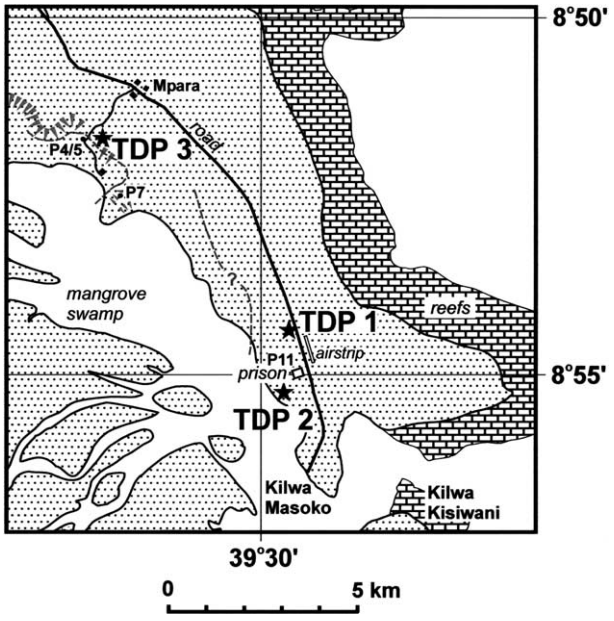

Fig. 5. Location map for TDP Sites 1–3 in the Kilwa area. P4/5, P7 and P11 represent planktonic foraminifer biozones of surface outcrop samples in the vicinity.

spread drift deposits across the Kilwa Masoko peninsula and is probably of Pliocene to Quaternary age. Drill cuttings showed that the sands have a maximum thickness of 4.5 m, after which pale olive clay was encountered in the cuttings slurry, mixed with quartz grains.

Core TDP1/2 contains a sandy, blue-grey clay (5B 7/1 to 5B 5/1), streaked and mottled with a yellowish orange sandy clay. A similar lithology occurs down to 12.95 m. The quartz grains within this blue-grey clay contrast with the overlying unconsolidated sands in being fine and angular. The fine quartz component is generally dispersed throughout the clay, but also forms distinct sandy clay beds which vary in thickness from 1 to 60 cm. Crude normal grading is sometimes visible within these. The yellow-orange streaks and mottles within the blue-grey clay unit are interpreted as the effects of modern weathering (similar to features seen near the surface in all the other holes drilled). Similar mottled blue-grey clays are exposed in cliffs to the east of Kilwa Masoko jetty (UTM 37L 557351, 9013005). We note also that outcrops of blue-grey clays in Kilwa Creek are marked on the Geological Survey map but are not now exposed. These clays are marked as Miocene in age and may correlate with the mottled blue-grey clays described here, although we found no biostratigraphic evidence with which to date them (see below).

From the top of Core 5 (14.10 m) to the bottom of the hole, the dominant lithology is entirely dark greenish-grey to greenish-black clays (5G 4/1 to 5G 2/1–N2) containing abundant calcareous microfossils of early Oligocene age (see below). It is concluded that a non-sequence is present at or around the core break between Cores TDP1/4 and 5. These dark greenish-grey to greenish-black clays contain fine quartz sand grains

Table 2
Intervals drilled and cored in TDP Site 1 (Kilwa Masoko 1, 8°54.516′S, 39°30.397′E)

Site	Core	Top (m)	Bottom (m)	Drilled (m)	Recovered (m)	Recovery (%)	Comment
TDP1	1	0.00	7.70	7.70	0.00	0	Interval drilled; cuttings only
	2	7.70	8.70	1.00	0.83	83	Short core
	3	8.70	11.10	2.40	2.40	100	Short core
	4	11.10	14.10	3.00	3.20	107	
	5	14.10	15.60	1.50	1.65	110	Short core
	5A	15.60	17.10	1.50	0.00	0	Interval drilled
	6	17.10	20.10	3.00	2.14	71	
	6A	20.10	25.30	5.20	0.00	0	Interval drilled
	7	25.30	28.10	2.80	3.56	127	
	8	28.10	30.60	2.50	1.10	44	
	9	30.60	33.40	2.80	2.88	103	
	10	33.40	36.40	3.00	2.84	94	
	11	36.40	39.40	3.00	2.45	82	
	12	39.40	42.90	3.50	3.20	91	
	13	42.90	46.30	3.40	3.20	94	
	14	46.30	49.30	3.00	2.68	89	
	15	49.30	52.30	3.00	3.14	104	
	16	52.30	55.30	3.00	3.10	103	
	17	55.30	58.30	3.00	1.82	61	
	18	58.30	61.30	3.00	1.58	53	
	19	61.30	64.30	3.00	3.32	111	
	20	64.30	67.30	3.00	1.78	59	
	21	67.30	70.30	3.00	0.88	29	
	22	70.30	74.10	3.80	1.39	36	

Total drilled: 74.10 m; total recovered: 49.14 m; recovery: 66.3%. Recovery may exceed 100% due to expansion of the cores and/or inaccuracies in measuring drilling depths.

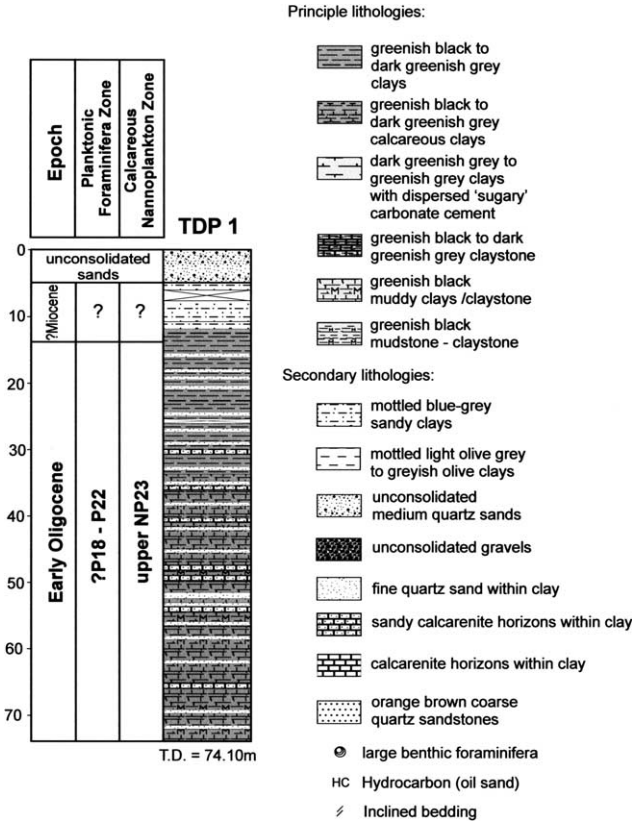

Fig. 6. Integrated litho- and biostratigraphy for TDP Site 1.

dispersed throughout, and fine laminations are frequently visible. Delicate burrow networks and pyrite cubes are visible sporadically. Some horizons with a higher concentration of quartz grains are discernable and rarely, within these, shelly fragments or small benthic foraminifers were observed with the hand lens. In the interval between 15 and 36 m depth, the clays are punctuated by two thin, but highly fossiliferous, calcarenite horizons. These included plant fragments, fenestral bryozoans and bivalves mixed in a general shell hash. These limestone coquinas and the repetitive fine sandy beds within the clays are suggestive of small sediment pulses being introduced from up-slope.

In Core TDP1/10, from a depth in the hole of 33.4 m downwards, the primary lithology of the clays is subtly different from above, with a muddy component discernable. In addition, the clays contains more conspicuous disseminated granular carbonate cement, particularly in the more sandy horizons.

The TOC, carbonate and sulfur content of nine samples from TDP Site 1 are shown in Table 3. TOC contents are very low in the upper blue grey clay (Sample TDP1/3-1, 19–32 cm), which appears oxidized, and range between 0.4% and 1.2% in the Oligocene clays, which are relatively organic rich. Variable carbonate contents reflect differences in microfossil concentration and minor calcite cementation.

Table 3
Results of geochemical analyses of samples from TDP Site 1

Sample	Depth (m)	$CaCO_3$ (%)	Sulfur (%)	TOC (%)
TDP 1/3-1, 19–32 cm	8.89–9.02	0.3	0.1	0.02
TDP 1/7-1, 87–100 cm	26.17–26.30	3.0	0.2	0.5
TDP 1/9-3, 60–71 cm	33.20–33.31	7.1	0.3	0.6
TDP 1/11-1, 39–50 cm*	36.79–36.90	3.2	1.0	0.8
TDP 1/13-2, 80–90 cm	44.70–44.80	13.5	0.2	0.8
TDP 1/14-1, 70–80 cm	47.00–47.10	4.2	0.7	0.8
TDP 1/16-2, 40–50 cm	53.70–53.80	4.0	0.1	0.7
TDP 1/20-2, 14–23 cm*	64.44–64.53	2.5	1.2	1.2
TDP 1/22-1, 23–32 cm	70.53–70.62	1.6	0.4	0.4

Samples highlighted with an asterisk were selected for biomarker study (see Table 1).

4.3. Planktonic foraminifers

Samples were processed from every core of TDP Site 1, but planktonic foraminifers were only found in Cores TDP1/9-11, TDP1/16 and TDP1/18. Even in these samples, specimens were very rare, with P:B ratios commonly much less than 1%. It is possible that the intervals between Cores TDP1/9-11 and TDP1/16-18 represent slightly deeper-water conditions than most of the rest of the site. When present, planktonic foraminifers are exceptionally well preserved, with glassy transparent tests and no evidence of calcite overgrowth or infilling.

The following taxa were identified: *Globigerina praebulloides* (Plate 1(3)–(4)), *Globigerina officinalis*, *Dentoglobigerina baroemoenensis*, *Globigerina ciperoensis* (Plate 1(5)), and *Globoturborotalita woodi* (Plate 1(1)). There is no noticeable change down core in this assemblage. The foraminifers indicate an Oligocene age which is consistent with the nannofossil evidence (see Section 4.4 below), although there are no biostratigraphic markers present.

4.4. Calcareous nannofossils

In the 29 samples studied, nannofossil abundance is very low throughout, with generally less than one specimen per field of view. Seven samples were barren. The nannofossil assemblages are relatively diverse, including 10 holococcolith species, and preservation is moderate to good. Cores TDP1/1 to TDP1/4 are barren, and Cores TDP1/15 to TDP1/22 yielded sparse and depauperate assemblages, with the exception of one relatively rich sample in Section TDP1/20-2.

The concurrent presence of *Lanternithus minutus* and *Sphenolithus distentus* below Core TDP1/4 indicates a stratigraphic level in the upper part of Zone NP23 (Martini, 1971) (lower Oligocene), also equivalent to the shorter Zone CP18 of Okada and Bukry (1980). This zonal designation is further supported by the presence of *Helicosphaera recta* (Plate 3(8)–(9)) (upper NP22-NN1), *Discoaster tanii ornatus* (Plate 4(10)) (NP21-23), and *Helicosphaera* cf. *H. carteri* (Plate 3(1)–(3)) (NP23-24) (Perch-Nielsen, 1985; de Kaenel and Villa, 1996).

4.5. Benthic foraminifers

Forty-two samples were studied for benthic foraminifers in TDP Site 1. Species diversity and abundance is high in the Oligocene greenish-black clay unit, and it is likely that many species are endemic and not previously described. There is a high abundance of *Ammonia beccarii*, as well as variety of species of *Quinqueloculina* (Plate 5(4)), *Pararotalia* (Plate 5(3)), *Nonion*, *Lenticulina* and *Cassidulina.* Planktonic: benthic ratios were not counted because of the extreme rarity or absence of planktonic foraminifers. Preservation varies from excellent to moderate through much of the samples to fair or poor in a few samples.

Species present include *Pararotalia mexicana*, *Cornuspira* sp. aff. *involvens*, *Lenticulina cultrata*, *Vulvulina pectinata*, *Triloculina austriaca*, *Rectuvigerina* sp. aff. *elegans* (Plate 5(1)), *Nummulites* sp. aff. *intermedius*, *Spiroloculina* sp. aff. *excavata*, *Bolivina* sp. aff. *budensis*, *Ampistegina* sp., *Ammonia beccarii*, *Ammonia annecten*, *Lenticulina inornata*, *Elphidium* sp., *Globorotalites* sp., *Pararotalia stellata*, *Heterostegina* sp., *Operculina* sp. and *Lepidocyclina* sp. Some of these taxa are illustrated in Plate 5.

Most of the benthic species present are long ranging, but have their last occurrences in the Oligocene. Species with their last occurrences in the Lower Oligocene are *Eggerella bradyi*, *Vulvulina pectinata*, *Vulvulina spinosa*, *Lenticulina cultrata*, *Lenticulina inornata*, and *Nummulites intermedius*, thus supporting the Early Oligocene age suggested by calcareous nannofossils. The rich assemblage of large benthic foraminifers is an indication of deposition of the sediments in a shallow marine paleoenvironment, which is supported by the presence of abundant echinoid spines, microgastropods, bivalves, and fish bones and teeth.

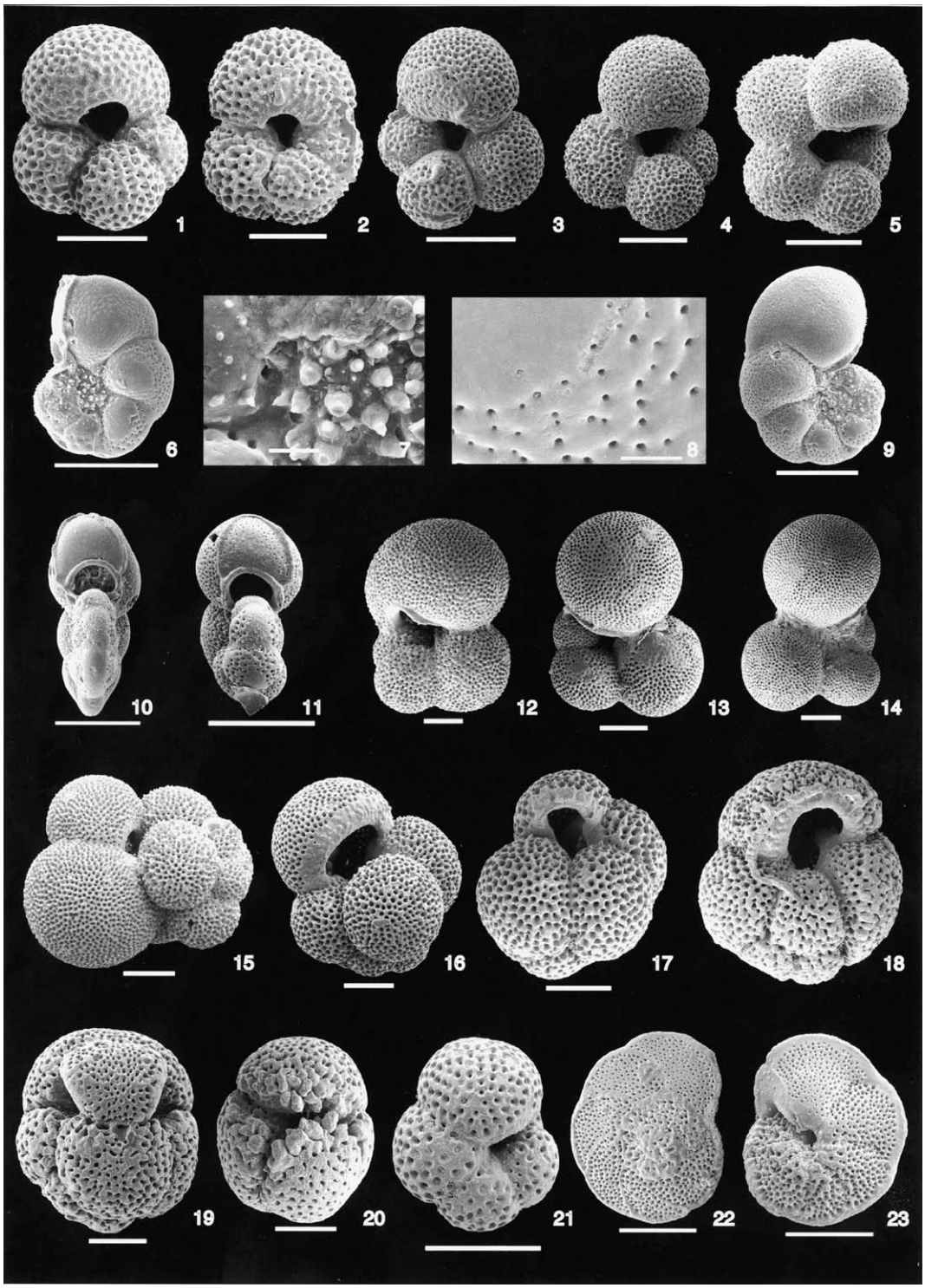

Plate 1. Selected planktonic foraminifers from TDP Sites 1 and 2. Scale bars = 100 μm, except enlargements (= 10 μm). (1) *Globoturborotalita woodi* (Sample TDP1/8/2, 21–33 cm); (2) *Globoturborotalita* sp. (Sample TDP1/8/2, 21–33 cm); (3) *Globigerina praebulloides* (Sample TDP1/11/2, 68–78 cm); (4) *Globigerina praebulloides* (Sample TDP1/10/3, 45–52 cm); (5) *Globigerina ciperoensis* (Sample TDP1/18/2, 0–10 cm); (6) *Pseudohastigerina* sp. (Sample TDP2/9/CC); (7) detail of umbilical ornamentation (same specimen as 6); (8) detail of chamber ornamentation (same specimen as 6); (9) *Pseudohastigerina* sp. (Sample TDP2/9/CC); (10) *Pseudohastigerina* sp. (Sample TDP2/9/CC); (11) *Pseudohastigerina micra* (Sample TDP2/9/CC); (12) *Subbotina crociapertura* (Sample TDP2/11/CC); (13) *Parasubbotina inaequispira* (Sample TDP2/25/CC); (14) *Parasubbotina eoclava* (Sample TDP2/32/1, 45–53 cm); (15) *Guembelitrioides nuttalli* (Sample TDP2/18/1, 20–26 cm); (16) *Guembelitrioides nuttalli* (Sample TDP2/9/CC); (17) *Guembelitrioides nuttalli–Globigerinatheka index* transition (Sample TDP2/17/2, 35–43 cm); (18) *Guembelitrioides nuttalli–Globigerinatheka index* transition (Sample TDP2/9/CC); (19) *Globigerinatheka* sp. (Sample TDP2/13/CC); (20) *Globigerinatheka senni*. (Sample TDP2/17/2, 35–43 cm); (21) *Paragloborotalia nana* (Sample TDP2/9/CC); (22) *Planorotalites capdevillensis* (Sample TDP2/1/2, 50–57 cm); (23) *Planorotalites capdevillensis* (Sample TDP2/1/2, 50–57 cm).

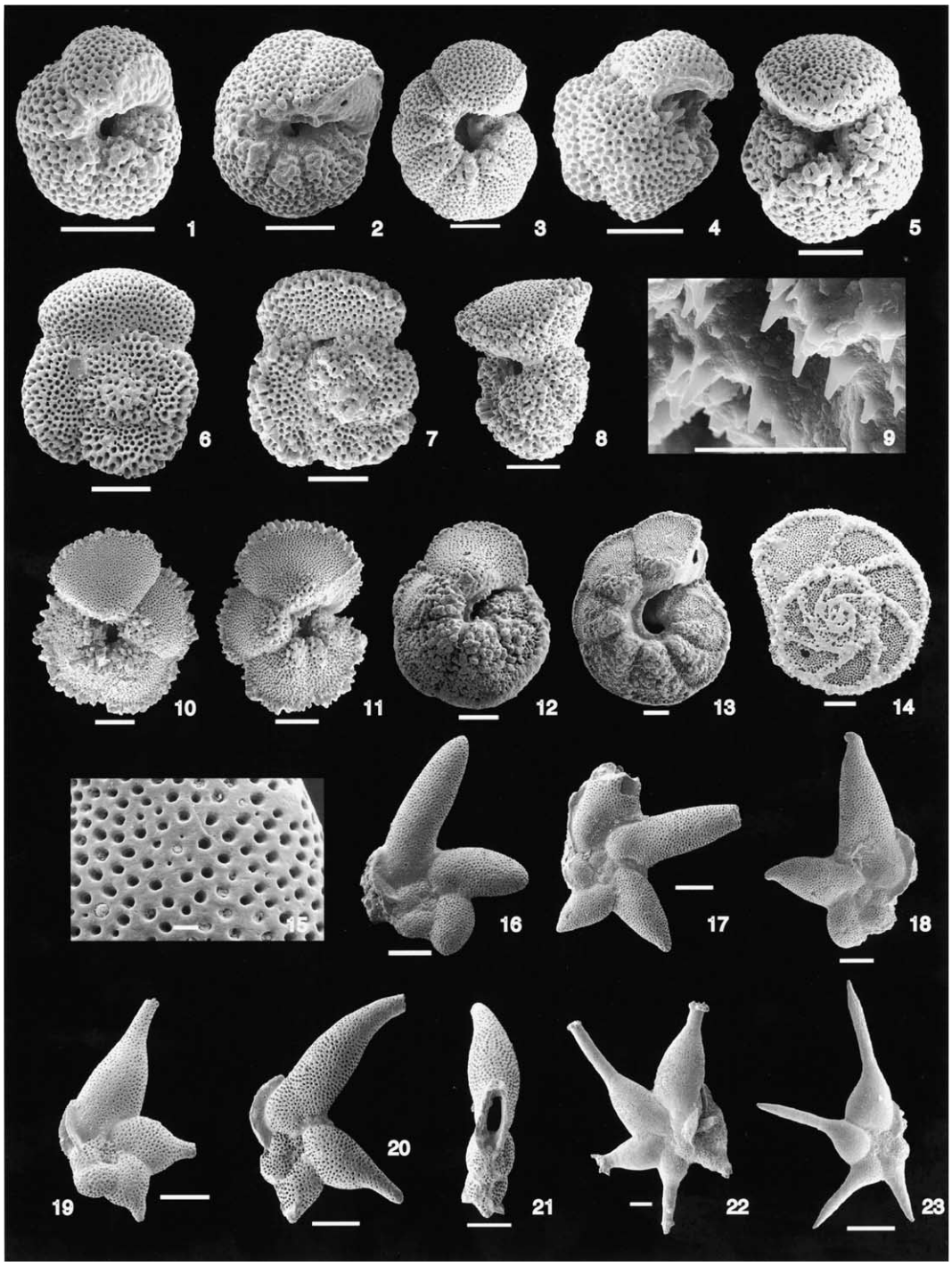

Plate 2. Selected planktonic foraminifers from TDP Site 2. Scale bars = 100 μm, except where given. (1) *Igorina lodoensis* (Sample TDP2/28/2, 16–24 cm); (2) *Igorina broedermanni* (Sample TDP2/13/CC); (3) *Igorina anapetes* (Sample TDP2/17/2, 35–43 cm); (4), *Acarinina* cf. *subsphaerica* (Sample TDP2/9/CC); (5) *Acarinina matthewsae* (Sample TDP2/9/CC); (6) *Acarinina matthewsae* (Sample TDP2/9/CC); (7) *Acarinina praetopilensis* (Sample TDP2/19/1, 10–20 cm); (8) *Acarinina praetopilensis* (Sample TDP2/9/CC); (9) detail of ultra-fine sub-micron murical ornamentation in apertural system (scale bar = 1 μm); (10) *Morozovella coronata* (Sample TDP2/1/2, 50–57 cm); (11) *Morozovella coronata* (Sample TDP2/2/1, 16–26 cm); (12) *Morozovella aragonensis* (Sample TDP2/17/2, 35–43 cm); (13) *Morozovella crater* (Sample TDP2/14/2, 1–31 cm); (14) *Morozovella crater* (Sample TDP2/3/CC); (15) Wall texture of transitional *Hantkenina* sp. (Sample TDP2/19/1, 90–100 cm); (16) *Clavigerinella caucasica* (Sample TDP2/23/1, 0–10 cm); (17) *Clavigerinella caucasica* (Sample TDP2/19/CC); (18) transitional *Hantkenina* sp. (Sample TDP2/22/1, 53–62 cm); (19) transitional *Hantkenina* sp. (Sample TDP2/18/1, 41–52 cm); (20) transitional *Hantkenina* sp. (Sample TDP2/18/2, 50–60 cm); (21) same specimen as 20, apertural view; (22) *Hantkenina mexicana* (Sample TDP2/4/2, 65–73 cm); (23) *Hantkenina liebusi* (Sample TDP2/5/1, 80–88 cm).

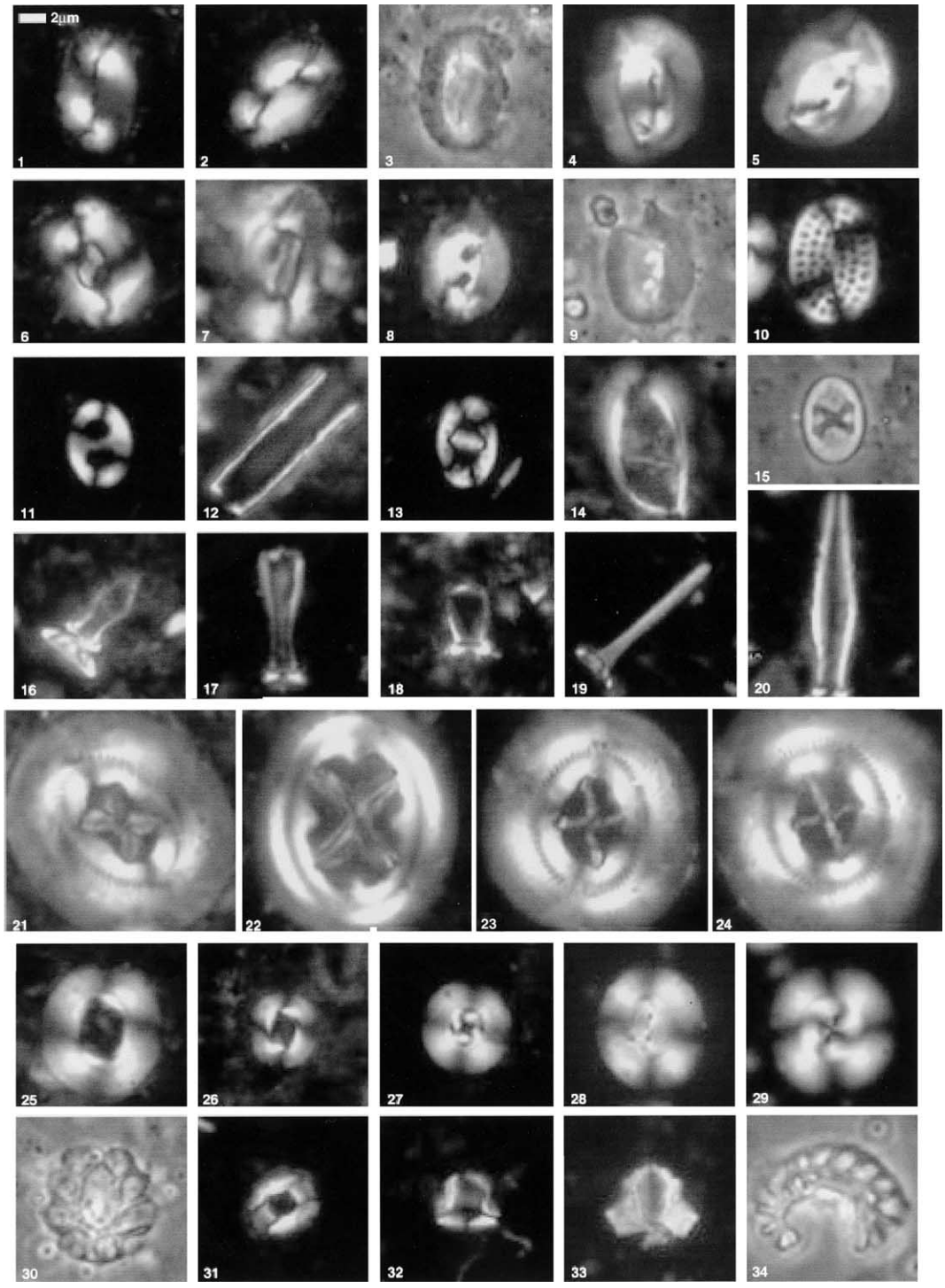

Plate 3. Selected calcareous nannofossils from TDP Sites 1–3. (1–3) *Helicosphaera* cf. *H. carteri*, Sample TDP1/14-1, 80 cm; (4–5) *Helicosphaera compacta*, Sample TDP1/20-2, 24 cm; (6) *Helicosphaera bramlettei*, Sample TDP2/15-1, 89 cm; (7) *Helicosphaera lophota*, Sample TDP2/17-1, 10 cm; (8, 9) *Helicosphaera recta*, Sample TDP1/7-3, 75 cm; (10) *Pontosphaera multipora*, Sample TDP2/7-1, 38 cm; (11) *Transversopontis rectipons*, Sample TDP3/19-3, 4 cm; (12) *Scyphosphaera columella*, Sample TDP2/13-1, 90 cm; (13) *Zygodiscus herlynii*, Sample TDP3/2-2, 64 cm; (14) *Lophodolithus acutus*, Sample TDP1/1-2, 56 cm; (15) *Neochiastozygus rosenkrantzii*, Sample TDP3/19-3, 4 cm; (16) *Blackites gladius*, Sample TDP2/17-1, 10 cm; (17) *Blackites herculeus*, Sample TDP3/12-1, 62 cm; (18) *Blackites moronium*, Sample TDP2/35-2, 49 cm; (19) *Blackites perlongus*, Sample TDP3/19-3, 4 cm; (20) *Blackites inflatus*, Sample TDP2/26-1, 32 cm; (21) *Chiasmolithus gigas*, Sample TDP2/24-1, 27 cm; (22) *Chiasmolithus grandis*, Sample TDP2/7-1, 38 cm; (23) *Coccolithus staurion*, Sample TDP2/9-1, 22 cm; (24) *Coccolithus staurion*, Sample TDP2/7-1, 38 cm; (25 and 26) *Reticulofenestra dictyoda*, Sample TDP1/1-2, 56 cm; 26; (27) *Cyclicargolithus floridanus*, Sample TDP1/13-3, 80 cm; (28) *Reticulofenestra bisecta*, Sample TDP4/7-1, 13 cm; (29) *Reticulofenestra reticulata*, Sample TDP4/1-1, 33 cm; (30) *Corannulus arenarius*, Sample TDP2/10-1, 6 cm; (31) *Lanternithus minutus*, Sample TDP1/14-1, 80 cm; (32) *Lanternithus minutus*, Sample TDP1/1-2, 56 cm; (33) *Orthozygus aureus*, Sample TDP1/20-2, 24 cm; (34) *Peritachelina ornata*, Sample TDP3/19-3, 4 cm.

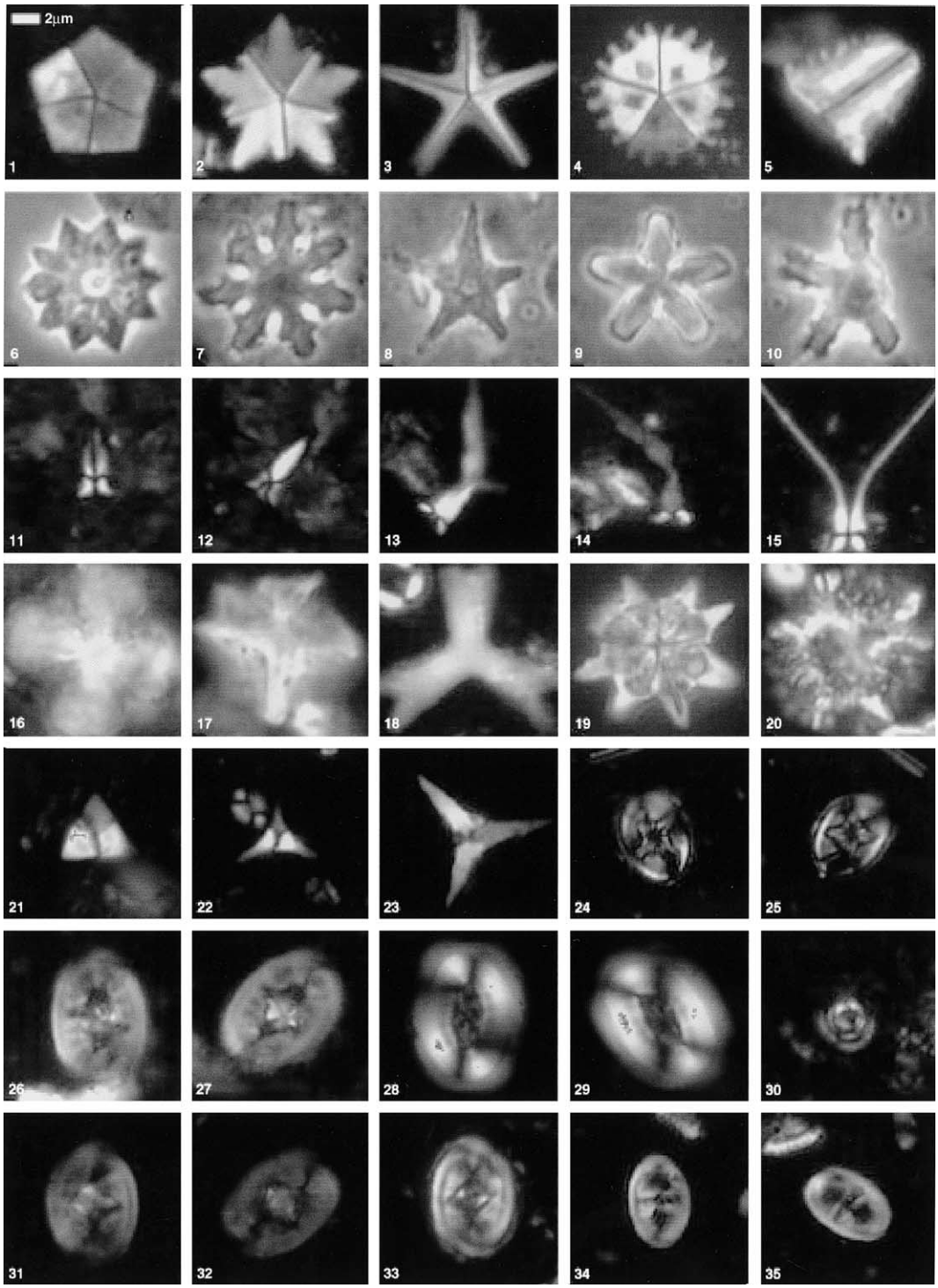

Plate 4. Selected calcareous nannofossils from TDP Sites 1–5. (1) *Braarudosphaera bigelowii*, Sample TDP3/19-3, 4 cm; (2) *Micrantholithus bramlettei*, Sample TDP3/19-3, 4 cm; (3) *Micrantholithus inaequalis*, Sample TDP3/19-3, 4 cm; (4) *Pemma papillatum*, Sample TDP4/7-1, 13 cm; (5) *Pemma papillatum*, Sample TDP4/1-1, 33 cm; (6) *Discoaster barbadiensis*, Sample TDP2/13-1, 90 cm; (7) *Discoaster nodifer*, Sample TDP2/7-1, 38 cm; (8) *Discoaster sublodoensis*, Sample TDP2/30-1, 11 cm; (9) *Discoaster tanii*, Sample TDP4/1-1, 33 cm; (10) *Discoaster tanii ornatus*, Sample TDP1/20-2, 24 cm; (11, 12) *Sphenolithus conspicuous*, Sample TDP3/2-2, 64 cm; (13, 14) *Sphenolithus distentus*, Sample TDP1/10-2, 76 cm; (15) *Spheholithus furcatolithoides*, Sample TDP2/17-1, 10 cm; (16) *Nanotetrina cristata*, Sample TDP2/23-1, 0 cm; (17) *Nannotetrina cristata*, Sample TDP2/3-1, 15 cm; (18) *Tribrachiatus orthostylus*, Sample TDP3/19-3, 4 cm; (19) ascidian spicules, Sample TDP1/20-2, 24 cm; (20) calcisphere, Sample TDP1/20-2, 24 cm; (21), *Uniplanarius trifidus*, Sample TDP5/9-1, 48–49 cm; (22) *Uniplanarius trifidus*, Sample TDP5/1-1, 60–61 cm; (23) *Uniplanarius trifidus*, Sample TDP5/1-1, 60–61 cm; (24, 25), *Eiffellithus parallelus*, Sample TDP5/1-1, 60–61 cm; (26, 27) *Reinhardtites anthophorus*, Sample TDP5/1-1, 60–61 cm; (28, 29), *Broinsonia parca constricta*, Sample TDP5/9-1, 48–49 cm; (30) *Cylindralithus*? *nieliae*, Sample TDP5/1-1, 60–61 cm; (31) *Reinhardtites levis*, Sample TDP5/9-1, 48–49 cm; (32) *Reinhardtites levis*, Sample TDP5/6-3, 36–37 cm; (33–35) *Tranolithus orionatus*, Sample TDP5/1-1, 60–61 cm.

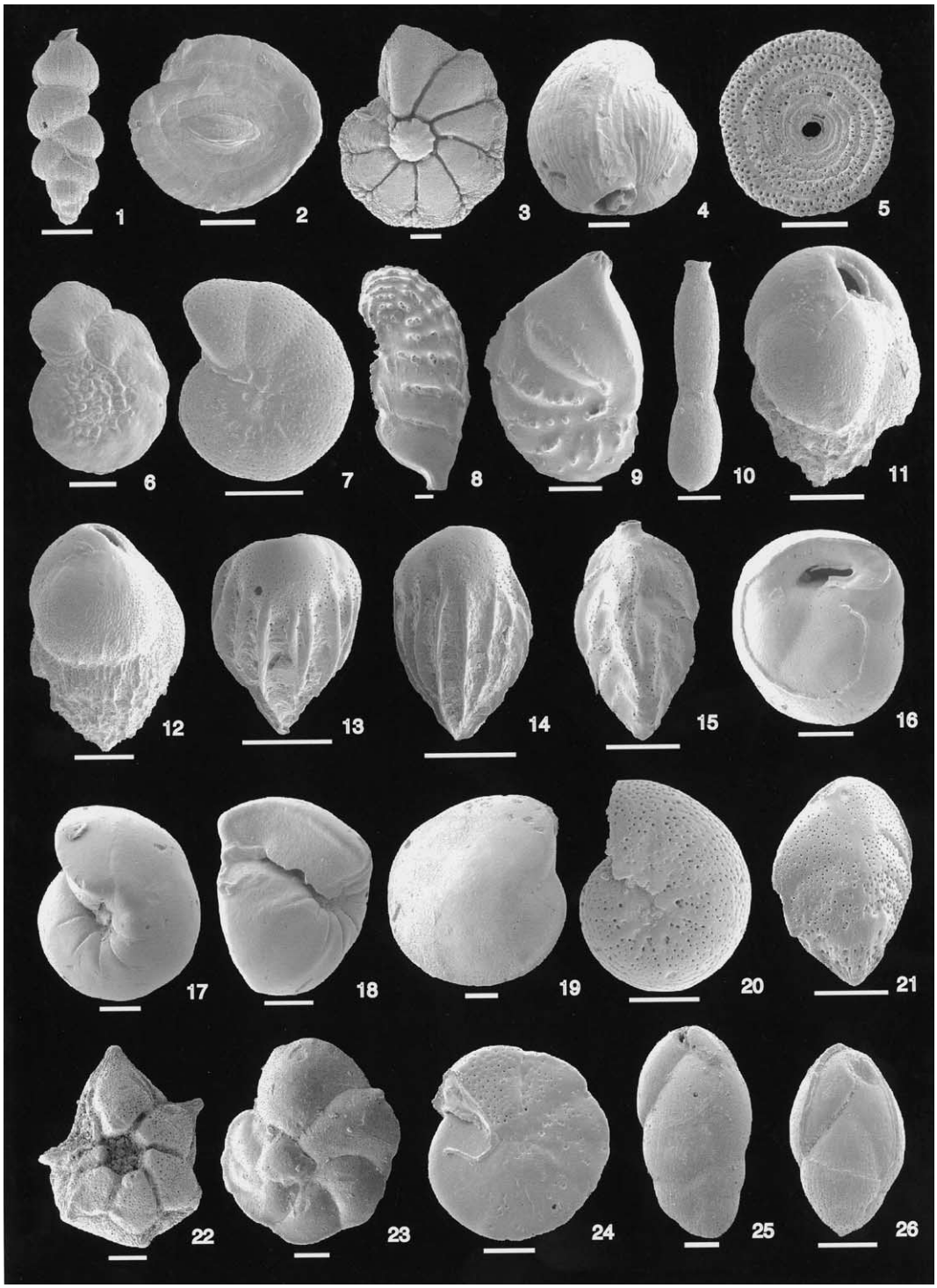

Plate 5. Selected benthic foraminifers from TDP Sites 1–4. Scale bars = 100 μm. (1) *Rectuvigerina elegans*, Sample TDP1/13-2, 78–80 cm; (2) ?*Ammodiscus* sp./*Spiroloculina* sp., Sample TDP1/13-2, 78–80 cm; (3) *Pararotalia* sp., Sample TDP1/7-2, 30–35 cm; (4) *Quinqueloculina* sp., Sample TDP1/7-3, 60–75 cm; (5), *Ammodiscus* sp., Sample TDP1/13-2, 78–80 cm; (6) *Planulina renzi*, Sample TDP2/3-1, 70–73 cm; (7) *Melonis* sp., Sample TDP2/3-1, 70–73 cm; (8) *Vaginulinopsis waiparaensis*, Sample TDP2/15-1, 86–90 cm; (9) *Astacolus* sp. Sample TDP2/19-2, 0–2 cm; (10) *Nodosaria longiscata*, Sample TDP2/19-2, 0–2 cm; (11) *Bulimina semicostata*, Sample TDP2/19-2, 0–2 cm; (12) *Bulimina* sp., Sample TDP2/19-2, 0–2 cm; (13) *Bulimina* sp., Sample TDP2/19-2, 0–2 cm; (14) *Bulimina alazanensis*, Sample TDP2/19-2, 0–2 cm; (15) *Trifarina* sp., Sample TDP2/16-1, 78–82 cm; (16) *Cassidulina cuneata*, Sample TDP2/16-1, 78–80 cm; (17) *Gyroidinoides* sp., Sample TDP2/16-1, 78–82 cm; (18) *Gyroidinoides* sp., Sample TDP2/16-1, 78–82 cm; (19) *Pseudonodosaria* sp., Sample TDP2/33-2, 30–33 cm; (20) *Melonis doreeni*, Sample TDP2/25-2, 48–53 cm; (21) *Aragonia zealandica*, Sample TDP2/25-1, 53–56 cm; (22) *Pararotalia* sp., Sample TDP4/3-1, 95–100 cm; (23) *Anomalinoides* sp., Sample TDP4/3-1, 95–100 cm; (24) *Cibicidoides* sp., Sample TDP3/5-1, 39–42 cm; (25) *Praebulimina* sp., Sample TDP3/5-1, 39–42 cm; (26) *Praebulimina* sp., Sample TDP3/5-1, 39–42 cm.

4.6. Palynology

Fourteen samples were studied for dinocysts and miospores. All samples were rich in terrestrial plant debris suggesting a relatively inshore, possibly estuarine or deltaic environment. Below Core TDP1/13, all samples studied were found to be barren of dinocysts, but above this level all samples contain rare palynomorphs (either dinocysts, miospores or both). Of these, Sample TDP1/6-1, 88–90 cm, Sample TDP1/9-3, 54–57 cm and Sample TDP1/13-2, 78–80 cm yielded a few long-ranging palynomorphs that are consistent with the Oligocene age suggested by calcareous nannofossils. These include the pollen species *Monoporites annulatus*, *Magnastriatites howardii*, and *Inaperturopollenites*, and the dinocysts *Lejeunecysta* sp. and *Systematophora* sp. Palynomorphs were mostly poorly preserved and partly pyritised.

4.7. Paleomagnetic analysis

Thirteen samples were taken for paleomagnetic analysis from relatively undisturbed intervals. The resulting data were not considered suitable for magnetostratigraphic interpretation because they are interpreted as having suffered remagnetization in diagenesis. Magnetizations are relatively weak, with natural remanent magnetizations varying between 1×10^{-2} and 2×10^{-5} A/m (most samples lie toward the lower end of this range). No systematic drilling-induced overprint is evident in demagnetization data, and a clear ChRM component can usually be identified. Stable paleomagnetic directions were identified for ~80% of the samples. While this represents a good success rate, it was found that the magnetic polarity data cannot be clearly correlated with the geomagnetic polarity timescale (GPTS) of Cande and Kent (1995) when plotted against depth and compared with age determinations from planktonic foraminifers and calcareous nannofossils. Similar results were obtained from TDP Sites 2 and 3 (see below). These sites all have different demagnetization characteristics compared to those from TDP Site 5. They usually have higher coercivities than would be expected for magnetite and they display irregular demagnetization characteristics or evidence for acquisition of a gyroremanent magnetization at AFs above 30 mT. The magnetization of some samples sharply decreases over a restricted range of AFs above 30 mT, which is characteristic of the presence of a narrow range of grain sizes in the single-domain size-range. These characteristics are typical of authigenic magnetic iron sulfide minerals, such as greigite (Sagnotti and Winkler, 1999), which commonly occurs in single domain sizes in anoxic sediments (Roberts, 1995). The abundance of pyrite in the TDP cores indicates that they were deposited under anoxic sulfate-reducing conditions, which is consistent with the inferred presence of greigite (or pyrrhotite). Greigite and pyrrhotite are being increasingly implicated with late diagenetic remagnetizations (e.g., Florindo and Sagnotti, 1995; Horng et al., 1998; Jiang et al., 2001; Weaver et al., 2002), and it seems likely that the magnetic polarity records from TDP Sites 1–3 have been compromised by a similar late diagenetic remagnetization.

4.8. Organic geochemistry

Two samples were selected for analysis of their saturated hydrocarbon, aromatic hydrocarbon, polar and acid fractions from TDP Site 1 (marked with an asterisk in Table 3). These were analyzed using GC and GC/MS (Fig. 7, see Table 1). In both cases, analyses of the saturated hydrocarbon fractions revealed predominantly C_{16}–C_{35} *n*-alkanes (Fig. 7A, Table 1), with C_{31} *n*-alkane (I; Fig. 4) being the most abundant component and an odd-over-even carbon-number predominance indicating a terrestrial origin (Eglinton and Hamilton, 1963, 1967). In addition, hopenes, predominantly C_{28} and C_{30} hop-17(21)-enes (II; Fig. 4) and hop-18(13)-enes and hopanes, predominantly 17β(H),21β homohopane (III; Fig. 4) and 17β(H),21β bishomohopane, all of bacterial origin (Ourisson et al., 1979), are abundant. In Sample TDP1/11-1, 39–50 cm, higher-molecular-weight hopanes are present. Also present, but in substantially lower abundances, are steranes, mainly ethylcholestane (IV; Fig. 4).

Analyses of the aromatic hydrocarbon fractions revealed substantial amounts of C_{25}–C_{35} *n*-alkanones (Fig. 7B and Table 1), especially C_{29} *n*-alkanone (V; Fig. 4), with an odd-over-even carbon-number predominance indicative of a terrestrial origin (Leif and Simoneit, 1995). In addition, Sample TDP1/20-2, 14–23 cm contains high abundances of polycyclic aromatic hydrocarbons (PAH), primarily picene (VI; Fig. 4).

Polar fractions are dominated by C_{16}–C_{32} *n*-alkanols (Fig. 7C, Table 1), with C_{28} *n*-alkanol (VII; Fig. 4) being the most abundant component and an even-over-odd carbon-number distribution, consistent with a terrestrial origin (Eglinton and Hamilton, 1963, 1967). Besides the *n*-alkanols, substantial amounts of higher-plant triterpenoids, predominantly friedelan-3-one (VIII; Fig. 4), are present; in fact, in Sample TDP1/20-2, 14–23 cm, friedelan-3-one (VIII) is the most abundant compound in the polar fraction. In addition, bacterial hopanoids, predominantly homohopan-29-one (IX; Fig. 4) and bishomohopan-31-one, are present. Steroids, especially 4,24-dimethylcholestan-3-one (X; Fig. 4) and 23,24-dimethyl-5α-cholestan-3-one or 24-ethyl-5α-cholestan-3-one, are also present but in substantially lower amounts. The last two can originate from multiple sources (Volkman et al., 1990), but in these sediments they most likely derived from higher-plant material. In contrast, 4-methyl steroids, like 4,24-dimethylcholestan-3-one

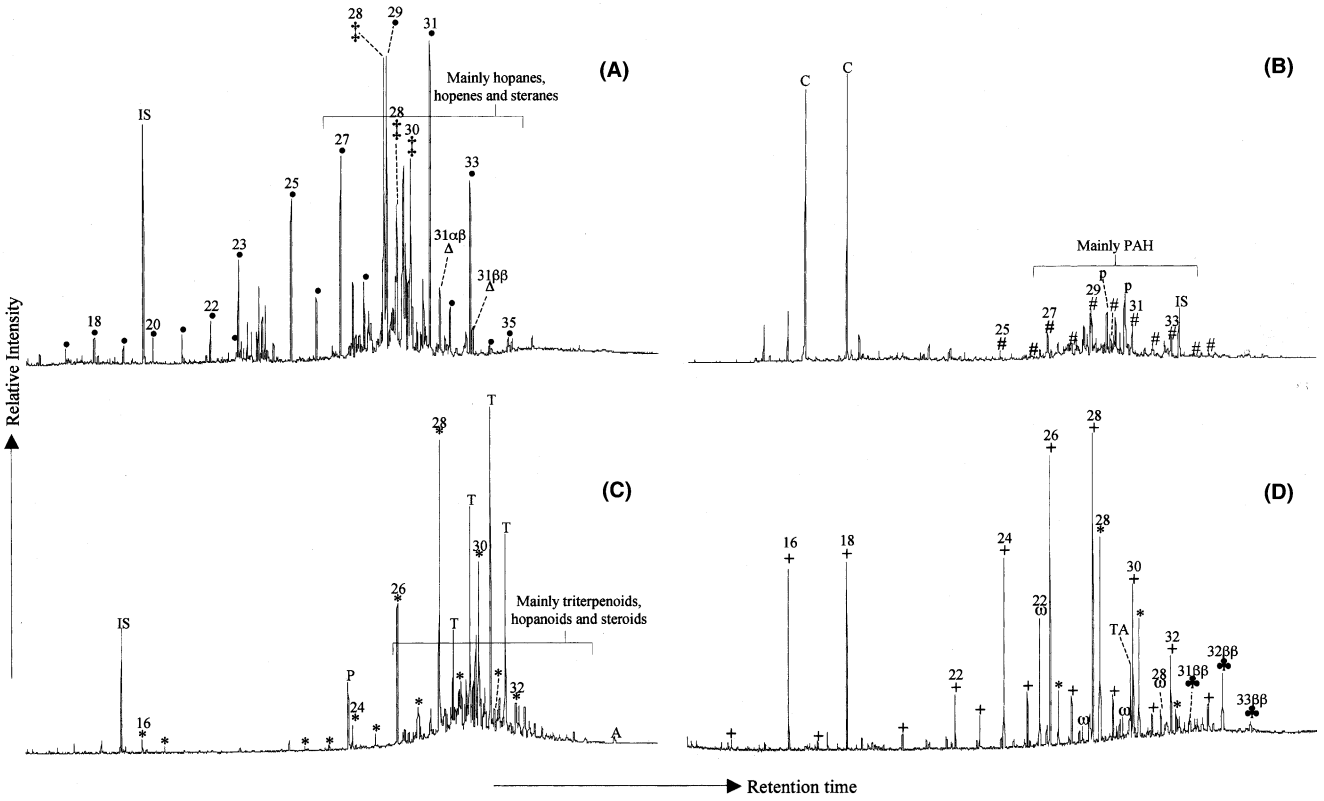

Fig. 7. Total ion currents of (A) the saturated hydrocarbon fraction, (B) the aromatic hydrocarbon fraction, (C) the polar fraction and (D) the acid fraction of Sample TDP1/20-2, 14–23 cm. ● = *n*-alkanes, ‡ = hopenes, △ = hopanes, # = *n*-alkenones, P = polycyclic aromatic hydrocarbons (PAH), ∗ = *n*-alkanols, T = triterpenoids, A = archaeol, + = *n*-alkanoic acids, ω = ω-hydroxy alkanoic acids, ♣ = hopanoic acids, TA = triterpenoic acids, IS = internal standard and C = contaminant. Numbers indicate carbon chain length and αβ or ββ indicates stereochemistry. The presence of *n*-alkanols in the acid fraction and the PAH in the polar fraction was due to an incomplete separation during column chromatography.

(X; Fig. 4) are thought to originate from dinoflagellates (Withers et al., 1978, Volkman et al., 1990, 1999), although a contribution from diatoms (Volkman et al., 1993) is also possible. Glycerol dipentadecyl diether (C_{15}–C_{15} diether; XI; Fig. 4) and archaeol (XII; Fig. 4) are also present, although in low amounts comparable to the steroids. The former compound is thought to derive from sulfate-reducing bacteria (Pancost et al., 2001), while archaeol is diagnostic for archaea (Kates et al., 1993; Koga et al., 1993).

Acid fractions are generally dominated by C_{16}–C_{34} *n*-alkanoic acids (Fig. 7D, Table 1), with C_{28} *n*-alkanoic acid (XIII; Fig. 4) being the most abundant component, and an even-over-odd carbon-number distribution consistent with a terrestrial origin (Eglinton and Hamilton, 1967). Substantial amounts of C_{22}-C_{32} ω-hydroxy alkanoic acids are also present, dominated by C_{22} ω-hydroxy alkanoic acid (XIV; Fig. 4) and with an even-over-odd predominance, again indicating a terrestrial origin (Eglinton and Hamilton, 1967, Holloway, 1982). Bacterial hopanoic acids, predominantly 17β(H),21β-bishomohopanoic acid (XV; Fig. 4), are abundant in both samples. In Sample TDP1/20-2, 14–23 cm, triterpenoic acids, predominantly 3,4-seco-friedelan-3-oic acid (XVI; Fig. 4), are also present.

In general, organic geochemical results indicate a high concentration of terrestrially-derived organic matter and very low thermal maturity.

4.9. Summary

Cores TDP1/1 to TDP1/5 consist of weathered blue-grey clays and unweathered greenish black clays, both of which are barren of calcareous microfossils. Similar barren blue-grey clays outcrop on the coast to the east of Kilwa Masoko town. Their age is unconstrained, except that they overlie the lower Oligocene unit below, and blue-grey Miocene clays, which may be part of the same formation, have previously been reported from the area by R. Stoneley (Moore et al., 1963). Unlike the Oligocene clays beneath, this barren unit is very low in organic carbon and has a lower calcium carbonate content than all other samples studied in this project. It may be a lacustrine deposit, possibly reworking the older clays of the area.

The rest of TDP Site 1 consists of relatively monotonous soft greenish-black to dark greenish-grey clays of lower Oligocene age (nannofossil zone NP23; 29.9–32.3 Ma). Benthic foraminifers from the Oligocene of TDP Site 1 are exceptionally well preserved and diverse. The

high abundance of benthic foraminifers in many samples, extreme rarity of planktonic foraminifers, and rarity of dinocysts indicates a shallow marine environment. Palynological slides are rich in terrestrial plant debris. Organic geochemical extracts reflect this high terrestrial input and also indicate a very low thermal maturity.

This relatively shallow-marine facies contrasts with the deeper-water Eocene deposits in the area (see Sections 5–7, below). This facies change may have developed due to a substantial eustatic sea level drop in the early Oligocene, related to the growth of the Antarctic ice cap, or may have been caused by regional uplift. The lack of macrofossils and rarity of bioturbation, plus the preservation of lamination and growth of pyrite in this shallow shelf setting suggests anoxic bottom water developed and persisted during deposition of the clays. A significant relative sea-level fall across the shelf may have left a series of restricted shallow lagoons which ponded the terrigenous clay influx and developed oxygen deficiency through lack of turnover in the water column. Further drilling may help constrain the timing of this regression.

The presence of a thick Oligocene formation on the Kilwa Masoko peninsula was unexpected, as such deposits do not crop out anywhere in the region (Moore et al., 1963; Schlüter, 1997). In the Lindi area further to the south, lower Oligocene deposits are mostly buff clays and limestones, which are quite unlike the facies described here. Horizontal to shallow-dipping middle Eocene sediments crop out about 1.5 km to the south and west of the drill site (see TDP Site 2, below). It is likely that a significant fault exists between TDP Sites 1 and 2.

5. TDP Site 2: Kilwa Masoko 2

5.1. Site selection

The area immediately behind Kilwa Masoko prison has long been known to yield excellently-preserved middle Eocene foraminifers. Two clay samples (Samples WA-1960 and WA-1963) were collected from this area some time before 1962 by W.G. Aitken of the Tanganyika Geological Survey, and the hantkeninids were described by Ramsay (1962), who concluded that the age was "lower and/or middle Eocene". A further sample of clay (Sample RS-24) was collected by R. Stoneley of BP-Shell Exploration Ltd., from a trench dug for a water pipe line ca. 200 yards west of Kilwa Masoko prison in 1954, and the foraminifers were described by Blow (1979) as belonging to Zone P11 (middle Eocene).

Sample RS-24, which is now held at the Natural History Museum in London became significant in foraminifer taxonomy when the following species were described from it for the first time by Blow (1979): *Globorotalia* (*Acarinina*) *broedermanni anapetes*, *Globorotalia* (*Acarinina*) *matthewsae*, *Globorotalia* (*Truncorotaloides*) *topilensis praetopilensis*, *Globorotalia* (*Morozovella*) *spinulosa coronata*, and *Globigerinita hardingae*.

The area was visited by us in 1998 and 1999. Although there is no exposure now in the pipeline trench, a number of samples of clays and limestones were collected from small outcrops and excavations in the area, some of which yielded excellently preserved foraminifers. The beds are flat-lying, so it is difficult to establish age-relationships between these surface outcrop samples. Nevertheless, all foraminifer assemblages contain both *Globigerinatheka* spp. and *Morozovella aragonensis*, indicating a position in Zone P11 (middle Eocene). One of our samples, Sample KIL99-41, was used for detailed stable isotope analyses as reported by Pearson et al. (2001).

TDP Site 2 was drilled on raised ground to the southwest of Kilwa Masoko prison, just outside the grounds of that institution (8°55.277′S, 39°30.219′E). The immediate area around the drill-site is littered with detached blocks of yellow-brown nummulitic limestone which show strong internal size-grading of the foraminifers, suggesting that they are derived from a hard, carbonate turbidite bed. It was expected that the site would spud in at a higher stratigraphic level than the Zone P11 outcrop samples that were collected in the prison grounds. However, the level was closely equivalent to the stratigraphic level of the prison outcrops, implying the existence of a small fault between TDP Site 2 and the prison, which may control the topography of the ridge on which TDP Site 2 was drilled. Coring was terminated at 92.78 m because of slow progress after the failure of the wireline coring system. A list of core depths is given in Table 4. A summary of the litho- and biostratigraphy is given in Fig. 8.

5.2. Lithostratigraphy

There is no unconsolidated drift cover at TDP Site 2, so after removing 0.7 m of topsoil, the drill string spudded-in directly on clays. Coring began immediately and encountered a discrete unit from 0.7 to 18.9 m depth of pale to greyish olive to light olive brown clay (10Y 5/2 with 5Y 5/6). These clays are mottled with dark yellowish orange clay. Dispersed fine carbonate grains occur throughout. There are also some minor gypsum laminae and gypsum-filled cavities developed in the lower portion of this unit. At a downhole depth of 2.7 m and again at 4.25 m, two beds of a hard dark yellowish-orange nummulitic coquina were cored. Blocks of these characteristic marker horizons are weathered out on the surface around the drill site, and also outcrop 200 m to

Table 4
Intervals drilled and cored in TDP Site 2 (Kilwa Masoko 2, 8°55.277′S, 39°30.219′E)

Site	Core	Top (m)	Bottom (m)	Drilled (m)	Recovered (m)	Recovery (%)	Comment
TDP2	0	0.00	0.70	0.70	0.00	0	Interval drilled
	1	0.70	2.30	1.60	1.65	103	Short core
	2	2.30	3.15	0.85	0.85	100	Short core
	3	3.15	6.15	3.00	0.92	31	
	4	6.15	8.00	1.85	2.13	115	Short core
	5	8.00	9.15	1.15	1.28	111	Short core
	6	9.15	10.20	1.05	1.36	130	Short core
	7	10.20	13.70	3.50	3.15	90	
	8	13.70	16.30	2.60	0.21	8	Most of core lost
	9	16.30	18.90	2.60	3.25	125	
	10	18.90	22.10	3.20	2.71	85	
	11	22.10	25.10	3.00	3.20	107	
	12	25.10	27.40	2.30	2.47	107	
	13	27.40	30.60	3.20	3.20	100	
	14	30.60	33.40	2.80	2.18	78	
	15	33.40	35.90	2.50	2.32	93	
	16	35.90	39.10	3.20	1.32	41	
	17	39.10	41.00	2.00	1.87	93	
	18	41.00	44.10	3.10	2.16	70	
	19	44.10	46.60	2.50	3.23	129	
	20	46.60	49.30	2.70	2.17	80	
	21	49.30	52.10	2.80	3.00	107	
	22	52.10	55.10	3.00	3.26	109	
	23	55.10	58.10	3.00	2.65	88	
	24	58.10	60.30	2.20	2.76	125	
	25	60.30	63.40	3.10	3.30	106	
	26	63.40	66.70	3.30	2.75	83	
	27	66.70	69.70	3.00	3.49	116	
	28	69.70	72.30	2.60	2.37	91	
	29	72.30	73.30	1.00	1.47	147	Short core
	30	73.30	76.30	3.00	3.35	112	
	31	76.30	79.40	3.10	3.10	100	
	31A	79.40	82.30	2.90	0.00	0	Core lost
	32	82.30	83.90	1.60	1.26	79	
	33	83.90	86.90	3.00	3.06	102	
	34	86.90	89.90	3.00	2.55	85	
	35	89.90	92.10	2.20	2.37	108	
	36	92.10	92.78	0.68	1.38	203	

Total drilled: 92.78 m; total recovered: 83.75 m; recovery: 90.3%.

the north-east around Kilwa Masoko prison. The coquina beds have sharp erosive bases and a crude size grading to the benthic foraminifers, suggesting they are turbiditic influxes from up-slope.

There is a sharp colour change in the clays at a depth of 18.9 m which is interpreted as an oxidation front. Below this level, and to the bottom of the hole, the principal lithology is greenish grey clay (5G 6/1 to 5G 4/1), finely laminated and containing occasional small burrows. The clays have a remarkably uniform colour throughout, varying between the lighter and darker end-members as a consequence of the localized concentration of carbonate cement grains, which lightens the colour. These carbonate grains commonly follow horizons containing a very fine quartz sand component, which could have increased primary porosity and permeability to pore fluids.

At a depth of 32 m, an 80 cm thick pale olive to yellowish grey (10Y 6/2 to 5Y 8/1), fine- to medium-grained calcarenite was cored. This is full of small benthic foraminifer tests (1–2 mm) set within a clay matrix which is well laminated and contains mini graded beds and cross lamination. Dark greenish grey clay rip-up clasts are also present. This suggests a turbiditic origin, which in this case entrained fragments of plastic clay over which the turbidity current travelled. The interval between 32 m and 45.6 m includes six similar turbiditic benthic foraminifer limestone horizons, separated by greenish grey to dark greenish grey clays as before. However, mixed in with this background sedimentation is a common component of benthic foraminifera and higher carbonate content, partially cementing it in places. This suggests that at least some reworking of shallower water sediment continued even between the

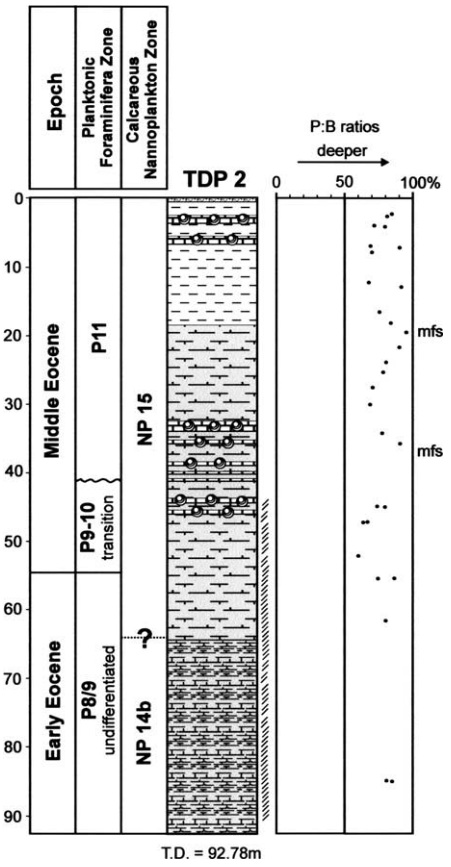

Fig. 8. Integrated litho- and biostratigraphy for TDP Site 2. Symbols are the same as for Fig. 7.

distinct turbiditic pulses which concentrated the benthic foraminifers in specific horizons. This thin 13.6 m unit may provide a useful lithostratigraphic marker for further studies in the area.

Microfossil assemblages midway through this unit demonstrate a stratigraphic gap (see Section 5.3, below). This seemingly corresponds to a hiatus of several million years, or a fault, and occurs between 39.25 m and 41.41 m depth. The limestone beds at 44.47 m and 45.3 m clearly demonstrate inclined bedding at an angle of about 25° and further evidence of inclined bedding is observed to the bottom of the hole.

Greenish-grey to dark greenish-grey clays continue uninterrupted from the base of the benthic foraminiferal limestone unit downwards to the bottom of TDP Site 2 at 92.78 m. From about 66 m down the granular carbonate content increase to give a more crumbly texture to the clays. There is also an overall increased abundance of bioturbation and the two factors together may indicate that this lower portion of TDP Site 2 was deposited in slightly shallower water depths.

The TOC and sulfur contents of the samples from TDP Site 2 range between 0.02% and 0.5% and 0.02% and 0.5%, respectively (Table 5), being generally lower than TDP Site 1. The carbonate contents range between 10.3% and 40.8% (Table 5), higher, on average, than values obtained for TDP Site 1. Certain levels contain abundant reworked shallow water carbonate debris, which probably accounts for some of the higher values obtained. In the bottom few cores, where the highest carbonate contents were recorded, calcite infillings of foraminifers were observed suggesting some diagenetic crystallization at those levels (see Section 5.3 below).

In order to establish which clay mineral groups are present, a suite of samples from TDP Site 2 were analysed using XRD. The results of these analyses were remarkably uniform. All of the clays are swelling clays. Stilpnomelane is the principal mineral group present, with minor quantities of secondary group minerals that were significantly altered, such as mica (muscovite), serpentine (disordered kaolinite and dickite) and quartz. Occasional chalcopyrite, carbonate-apatite and faujasite are also represented in some samples, but no patterns to their

Table 5
Results of geochemical analyses of samples from TDP Site 2

Sample	Depth (m)	$CaCO_3$ (%)	Sulfur (%)	TOC (%)
TDP 2/2-1, 6–16 cm	3.36–3.46	10.6	0.2	0.2
TDP 2/4-2, 50–65 cm	7.65–7.80	13.8	0.3	0.1
TDP 2/6-2, 4–14 cm	10.19–10.29	11.1	0.3	0.02
TDP 2/9-1, 24–35 cm	16.54–16.63	13.9	0.02	0.2
TDP 2/10-3,16–30 cm*	21.06–21.20	10.5	0.5	0.5
TDP 2/13-1,78–90 cm	28.18–28.30	10.3	0.3	0.2
TDP 2/15-1, 73–85 cm	34.13–34.25	11.5	0.2	0.3
TDP 2/17-2, 44–59 cm	40.54-40.69	13.0	0.1	0.2
TDP 2/19-2, 15–21 cm	45.25–45.31	15.6	0.1	0.3
TDP 2/22-1, 38–51 cm	52.48–45.61	30.1	0.04	0.3
TDP 2/24-3, 3–18 cm	60.13–60.28	21.3	0.02	0.3
TDP 2/25-2, 53–60 cm*	61.83–61.90	21.4	0.5	0.2
TDP 2/27-2, 8–18 cm	67.78–67.88	14.7	0.1	0.3
TDP 2/30-3, 105–114 cm	76.35–76.44	38.3	0.02	0.5
TDP 2/33-2, 38–51 cm	85.28–85.41	40.8	0.1	0.4

Samples highlighted with an asterisk were selected for biomarker study (see Table 1).

occurrence are discernable. There is no variation in clay mineralogy across the early-middle Eocene boundary.

5.3. Planktonic foraminifers

A total of 53 samples from TDP Site 2 were studied for planktonic foraminifers. Assemblages are diverse and abundant, and include members of the deep-dwelling plankton, indicating a relatively deep-water, outer-shelf environment.

Foraminifer shells frequently show orange surficial oxide staining down to the lower part of Core TDP2/9 (about 18.0 m), presumably because of oxidation in proximity to the modern land surface. Below this, pyrite is frequently encountered and, in some samples (e.g. in Core TDP2/24), it is abundant. In general, assemblages are diverse and excellently preserved, with no sign of diagenetic recrystallization, although calcite infillings occur in certain intervals and are common below Core TDP2/29. The excellent preservation in most samples (see Plates 1 and 2) means that the material is suitable for geochemical analysis.

From the surface down to Sample TDP2/17-1, 15–25 cm the assemblages indicate planktonic foraminifer Zone P11 (middle Eocene). Stratigraphically useful taxa include *Morozovella aragonensis* (Plate 2(12)), *Morozovella coronata* (Plate 2(10–11)), *Morozovella spinulosa*, *Turborotalia frontosa*, *Turborotalia possagnoensis*, *Globigerinatheka index*, *Globigerinatheka* cf. *subconglobata* and *Hantkenina mexicana* (Plate 2(22)). The first appearance of *Hantkenina liebusi* (Plate 2(23)) is in Sample TDP2/13-CC, although it only occurs frequently above Sample TDP2/9-2, 85–89 cm. This datum may prove a useful subdivision for Zone P11.

Between Samples TDP2/17-1, 15–25 cm and TDP2/18-1, 41–52 cm there is a marked change in planktonic foraminifer assemblages. Globigerinathekids are absent below this level. The interval from Sample TDP2/18-1, 41–52 cm to TDP2/23-1, 0–10 cm is characterized by hantkeninids that are transitional in morphology between *Clavigerinella caucasica* and *Hantkenina mexicana* (Plate 2(16–21)). Such forms are very rare and have previously been described only from Austria (see Coxall et al., 2003 for discussion). A detailed account of this evolutionary transition will be published elsewhere.

The most obvious interpretation of this change in assemblage is that there is a hiatus cutting out almost all of Zone P10. The interval directly beneath, which contains the transitional hantkeninids described above, is correlated to the uppermost part of Zone P9, although the index fossil for that zone (*Astrorotalia palmerae*) is absent from the core. In this interpretation, the hiatus corresponds to a gap of several million years. It also corresponds roughly to the onset of inclined bedding in the core which was observed in Cores TDP2/18 downwards (see above).

Just below the first appearance of transitional hantkeninids is the first appearance of *Clavigerinella* in Sample TDP2/23/2, 10–20 cm. Below this, hantkeninids are absent. Several other species are present, however, that do not occur in the upper part of the site. These include *Morozovella marksi*, *Morozovella caucasica*, *Acarinina cuneicamerata*, *Parasubbotina inaequispira* (Plate 1(13)), *Parasubbotina griffinae*, and *Parasubbotina eoclava* (Plate 1(14)). These observations support the evidence for a stratigraphic gap in the site.

A potentially useful zone-fossil for the early to middle Eocene transition is the first occurrence of *Guembelitrioides nuttalli* (= *higginsi* of some authors) (Plate 1(15–16)). Forms without supplementary apertures appear in Sample TDP2/25CC. Also of note is that occurring continuously below Sample TDP2/23/2, 10–20 cm is a nondescript species of *Pseudohastigerina* that possesses compressed chambers, an imperforate band around the periphery and imperforate areas on the umbilical shoulders of the chambers.

In summary, the upper part of the core is assigned to Zone P11, and exhibits subtle changes in the assemblages up core. A sharp hiatus in Core TDP2/17 cuts out the lowermost part of Zone P11 and almost all of P10, beneath which is a rarely sampled stratigraphic interval that spans the P9–P10 boundary (corresponding roughly to the Ypresian–Lutetian boundary). Beneath this level, samples are assigned to Zone P8/P9 undifferentiated because of the absence of the zone-fossil *A. palmerae*, although they probably correlate with the upper part of Zone P9.

Although the planktonic foraminifer evidence seems very strong, the suggestion of a large hiatus in Core TDP2/17 is opposed to some extent by the nannofossil evidence (see below), in which the interval above and below the supposed hiatus is placed in nannofossil Zone NP15a.

5.4. Calcareous nannofossils

Twenty-five samples were studied, and all yielded rare to abundant, diverse nannofossil assemblages of moderate to good preservation. The assemblages are notably rich in rhabdoliths, holococcoliths, pontosphaerids and pentaliths, all considered to be indicators of shelf environments (Perch-Nielsen, 1985; Aubry, 1999). However, most middle Eocene taxa are also represented in the samples, and total species richness from the section is 158 species; remarkably high for this fossil group.

The section ranges from Subzones NP14b to NP15c (Martini, 1971; Aubry, 1991) (Middle Eocene). *Blackites inflatus* is the zonal marker for Subzone NP14b and is present from Core 35 to 26 (Plate 3(20)). Some authors claim this species is restricted to NP14b (Varol, 1989; Aubry, 1983), while others have it ranging slightly higher (Perch-Nielsen, 1985). The base of Zone NP15

could not be precisely identified due to the absence of the index-taxon *Nannotetrina fulgens*. However, other species of the genus (e.g. *Nannotetrina cristata* Plate 4(17)) were recorded from Cores 26 to 2, albeit in low numbers. The last occurrence of *Discoaster sublodoensis* (Plate 4(8)) is placed just below the first occurrence of *N. fulgens* in the Lyle et al. (2002) timescale, and therefore approximates the base of NP15; this event is recorded in Core 26.

Subzone NP15b is defined by the total range of *Chiasmolithus gigas* (Plate 3(21)), a species that is present, although rarely, from Sample 24-2, 27 cm to 10-1, 6 cm. Questionable *C. gigas* specimens were recorded up to Core 2, but were logged as *Cruciplacolithus staurion* (with rotated crosses). The NP15b Subzone may therefore range as high as Core 2. The presence of *Blackites gladius* (Plate 3(16)) at the top of the section indicates an age no younger than Subzone NP15c. Possible conflicts with the planktonic and benthic foraminifer biostratigraphy are discussed in Section 5.9 below.

5.5. Benthic foraminifers

A total of 54 samples were analyzed for benthic foraminifers from TDP Site 2. Species abundance and diversity is very high (see Plate 5). P:B ratios are high, indicative of deposition in deep shelf waters. Preservation is excellent to moderate, with some levels being subject to calcite infillings. The lower to middle Eocene age is confirmed by the presence of *Nummulites laevigatus*, *Aragonia aragonensis*, *Aragonia tenera*, *Neoeponides karsteni*, *Cibicidoides truncanus*, *Spiroloculina canaliculata*, *Marginulina gutticostata*, *Marginulinopsis fragraria*, *Bulimina alazanensis* (Plate 5(14)), *Cibicidoides eocaenus*, *Uvigerina havanensis*, *Cibicides westi*, *Lenticulina gutticostata*, *Lagena striata*, *Spiroplectammina lanceolata*, *Dentalina deflexa*, *Bulimina impedens*, *Hoeglundina elegans* including other common Middle Eocene species of *Angulogavelinella*, *Stilostomella*, *Trifarina*, *Bathysiphon*, *Aragonia*, and *Osangularia*.

The presence of *Bulimina impedens*, *Rectouvigerina elegans* and *Pararotalia stellata* from Cores TDP2/1 to TDP2/17 confirm the age as middle Eocene. These species have their last occurrences in middle Eocene planktonic foraminifer Zone P11. The presence of *Uvigerina havanensis*, *Aragonia zealandica* and *Cibicidoides perlucida* in cores TDP2/18–TDP2/21 indicates a stratigraphic level equivalent to planktonic foraminifer zones P9–P10.

A down core increase in the species diversity of *Neoflabellina* was observed in Cores TDP2/18-21, which may be related to the stratigraphic gap detected with planktonic foraminifers. Cores TDP2/23-TDP2/35 have high abundance of *Aragonia aragonensis* (P8–P12), *Rzehakina epigona* (P10), *Bulimina callahani* (P10), *Aragonia zealandica* and new forms of *Aragonia* sp., *Tristix*, *Plectofrondicularia*, *Spiroloculina*, *Spiroplectammina* and *Trifaria*. *Dorothia* and *Marssonella* are also abundant in these levels and *Cibicidoides micrus* and *Bulimina semicostata* were observed only below this level.

5.6. Palynology

Fifteen samples were studied from TDP Site 2 for palynology. All samples studied contain dinocysts and miospores. Dinocysts were generally common to abundant between Cores TDP2/10 and TDP2/22. A decrease in abundance of dinocysts and chorate cysts, and an increase in abundance of miospores, was observed up core between this level and Core TDP2/8, possibly indicating a shallowing of the environment. The stratigraphically significant taxa, with their age-ranges as given in the literature include *Polysphaeridium biformum* (middle Eocene) (Plate 6(10)), *Operculodinium ornamentum* (middle Eocene), *Homotryblium oceanicum* (middle Eocene) (Plate 6(2)), *Homotryblium abbreviatum* (early–middle Eocene) (Plate 6(6)), *Glaphyrocysta intricata* (middle Eocene), *Homotryblium aculeatum* (Eocene) (Plate 6(7)), *Diphyes ficusoides* (middle Eocene) (Plate 6(3)) and *Areosphaeridium diktyoplokum* (Eocene) (Plate 6(5)).

5.7. Paleomagnetic analysis

Fifty samples were taken for paleomagnetic analysis from relatively undisturbed intervals in TDP Site 2. As at TDP Site 1, the resulting data were not considered suitable for magnetostratigraphic interpretation because of probable remagnetization in early diagenesis (see Section 4.7 above).

5.8. Organic geochemistry

The compounds in the saturated hydrocarbon fractions have distributions similar to those from TDP Site 1 (Table 1). Sample TDP2/10-3, 16–30 cm is distinct from both Sample TDP1/11-1, 39–50 cm and Sample TDP2/25-2, 53–60 cm in that C_{28} hop-13(18)-ene is the most abundant component present and hopenes are particularly abundant. In addition, the C_{29} *n*-alkane is the most abundant *n*-alkane present and not the C_{31} *n*-alkane (as in the case of the TDP Site 1 saturated hydrocarbon fractions). The aromatic hydrocarbon fractions contain no *n*-alkanones or PAHs. The TDP Site 2 polar fractions contain, like those of TDP Site 1, predominantly *n*-alkanols, although the C_{30} *n*-alkanol is the most abundant *n*-alkanol. In addition, substantial amounts of hopanoids, the C_{15}/C_{15} diether (XI; Fig. 4) and archeol (XII; Fig. 4) and low abundances of steroids and triterpenoids are present. The distribution of acids in Sample TDP2/10-3, 16–30 cm is comparable to that of the TDP Site 1 acid fractions, with substantial amounts

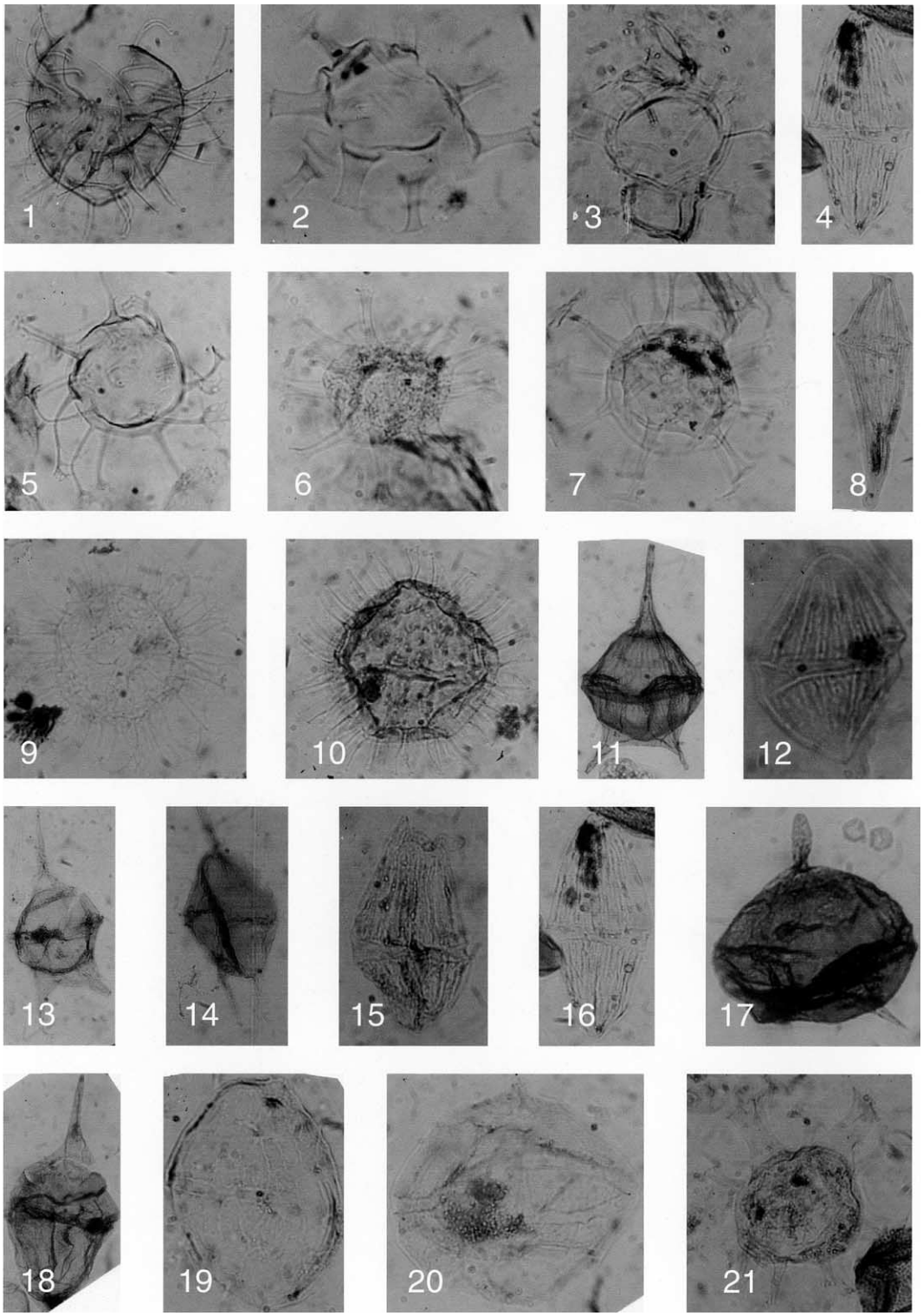

Plate 6. Selected palynomorphs from TDP Sites 1–5. Magnifications are variable. (1) *Cordosphaeridium brevispinum*, Sample TDP2/15-1, 86–90 cm; (2) *Homotryblium oceanicum*, Sample TDP2/22-2, 3–5 cm; (3) *Diphyes ficusoides*, Sample TDP2/20-2, 3–5 cm; (4) *Dinogymnium westralium*, Sample TDP5/7-1, 49–54 cm; (5) *Areosphaeridium diktyoplokum*, Sample TDP2/20-2, 3–5 cm; (6) *Homotryblium abbreviatum*, Sample TDP2/15-1, 86–90 cm; (7) *Homotryblium aculeatum*, Sample TDP2/18-1, 73–77 cm; (8) *Dinogymnium longicorne*, Sample TDP5/3-1, 26–30 cm; (9) *Enneadocysta arcuatum*, Sample TDP4/1-2, 23–25 cm; (10) *Polysphaeridium biformum*, Sample TDP2/15-1, 86–90 cm; (11) *Cerodinium striatum*, Sample TDP5/7-1, 49–54 cm; (12) *Alisogymnium downiei*, Sample TDP5/11-2, 51–56 cm; (13) *Cerodinium granulostriatum*, Sample TDP5/8-1, 85–90 cm; (14) *Ceratiopsis diebelii*, Sample TDP5/8-1, 85–90 cm; (15) *Dinogymnium acuminatum*, Sample TDP5/8-1, 85–90 cm; (16) *Dinogymnium westralium*, Sample TDP5/7-1, 49–54 cm; (17) *Senegalinium bicavatum*, Sample TDP5/7-1, 49–54 cm; (18) *Andalusiella mauthei*, Sample TDP5/3-1, 26–30 cm; (19) *Subtilisphaera* sp., Sample TDP5/10-/3, 44–49 cm; (20) *Trichodinium bifurcatum*, Sample TDP5/6-2, 60–64 cm; (21) *Callaiosphaeridium asymmetrica*, Sample TDP5/7-1, 49–54 cm.

of *n*-alkanoic acids and ω-hydroxy alkanoic acids and lesser amounts of hopanoic acids and triterpenoic acids. In addition, and distinct from TDP Site 1 sediments, substantial amounts of C_{23}–C_{30} α-hydroxy alkanoic acids are also present. Similar to the ω-hydroxy alkanoic acids, α-hydroxy alkanoic acids have an even-over-odd carbon-number predominance, indicating a terrestrial origin (Eglinton and Hamilton, 1967).

5.9. Summary

All cores from TDP Site 2 are dominated by clays that are interpreted as having been deposited in an outer shelf environment. An oxidation front occurs at about 18.9 m. Above this, the principal colour is olive brown clay; below it is dark greenish-grey clay. Occasional limestone beds consist of allochthonous material from shallow water, especially larger foraminifers, and are interpreted as having been introduced by turbidity currents. Planktonic foraminifer assemblages are diverse and fully marine in character, including deep-dwelling species, and many of them are beautifully preserved. Nannofossil assemblages are very diverse and dominated by continental shelf species. P:B ratios are generally high (60–90%) indicating a deep shelf environment. Variations in these, together with down hole changes in dinocyst and miospore assemblages, may be related to subtle changes in water depth.

Although the planktonic foraminifers and calcareous nannofossils both indicate a middle Eocene age, there is a considerable mismatch between the two zonations. Results from the two fossil groups agree in placing the topmost cores in Zone P11 and Zone NP15, both consistent with an age of about 44 Ma. However, the planktonic foraminifers suggest a significant age gap in Core TDP2/17, beneath which sediments of the P9–10 transition interval indicate an age of about 49 Ma. This possible hiatus level corresponds approximately to the onset of observed inclined bedding in the core. Subtle changes in benthic foraminifer assemblages support this interpretation. The nannofossils, on the other hand, do not show evidence of a large hiatus, in that sediments immediately above and below this level are both assigned to Subzone NP15a (46.1–47.3 Ma). The bottom of the drill-site is assigned to planktonic foraminifer Zone P8/P9 (undifferentiated—but probably correlative with the upper part of Zone P9, about 49.5 Ma), whereas the nannofossils are assigned to Subzone NP14b (47.3–48.5 Ma). Both the nannofossil and foraminifer evidence are robust and supported by the presence of a variety of taxa. We suggest that the correlation of these zonal schemes may need to be revised for shelf sediments. Possibly the zone-fossil for NP14b, *Chiasmolithus gigas*, may have had an extended range on the shelf.

The hiatus suggested by the foraminifers seems to correspond to an abrupt change in dip downhole. These factors together may suggest either that an angular unconformity exists, corresponding to most of Zone P10, or that the core penetrated through a fault plane into a rotated block below. Neither explanation is entirely satisfactory. There is no change in lithology either side of the proposed hiatus and yet tectonic activity would be required to fold the underlying beds prior to recommencement of deposition. With the fault hypothesis, a normal fault would be needed to cut out P10, but it would be difficult to achieve this without tilting the overlying block as well. A third option is that during a break in sedimentation that corresponded to P10, there was some degree of soft sediment deformation on the deeper shelf, including slumping of clays. This would produce a variety of gently dipping, rotated slump blocks over which sedimentation could resume. Destabilisation of shallower unconsolidated sediment, such as benthic foraminifer sands, might also have led to the thin turbidite coquina horizons present at this level.

The organic geochemistry of TDP Site 2 reveals a predominance of terrestrial biomarkers indicating a substantial fluvial input to the shelf, and also a very low degree of thermal maturity similar to the other sites drilled. The clay mineralogy is predominantly stilpnomelane, but also contains mature secondary-group minerals that had experienced significant alteration. This is consistent with reworking of these clays and it seems likely that the source for much of the clay sediment in the Kilwa area during the Paleogene was previously deposited Mesozoic clays exposed by sea-level fluctuations.

6. TDP Site 3: Mpara Hill

6.1. Site selection

TDP Site 3 was drilled in open scrub to the south-east of a small track leading from the main Kilwa Masoko road to the coast, north of Ras Pungunyuni (8°51.585′S, 39°27.655′E). Surface outcrop samples collected by the track nearby indicates an upper Paleocene age (Zone P4–5; Sample PP98K-15), while further to the south, sediments of P7 age (lower Eocene) have been collected (Sample PP98K-16). As expected, the drill-site was spudded in on lower Eocene sediments (Zone P6b) allowing the sampling of one of the supposedly warmest climatic intervals of the Cenozoic. Coring was terminated at 56.4 m when it became apparent that the lower part of the site was tectonically disturbed, showed inclined bedding, and microfossil preservation from below 47 m was not as good as higher in the core. A list of core depths is given in Table 6. A summary of the litho- and biostratigraphy is shown in Fig. 9.

Table 6
Intervals drilled and cored in TDP Site 3 (Mpara Hill, 8°51.585′S, 39°27.655′E)

Site	Core	Top (m)	Bottom (m)	Drilled (m)	Recovered (m)	Recovery (%)	Comment
TDP3	0	0.00	6.90	6.90	0.00	0	Interval drilled
	1	6.90	9.90	3.00	2.51	84	
	2	9.90	12.90	3.00	3.14	105	
	3	12.90	13.90	1.00	0.13	13	Most core lost
	4	13.90	16.90	3.00	2.98	99	
	5	16.90	18.90	2.00	1.95	97	
	6	18.90	23.40	4.50	1.28	28	
	7	23.40	26.40	3.00	1.72	57	
	8	26.40	29.10	2.70	0.83	30	
	9	29.10	30.70	1.60	0.89	56	
	10	30.70	33.65	2.95	1.00	34	
	11	33.65	36.80	3.15	1.57	50	
	12	36.80	41.40	4.60	1.89	41	
	13	41.40	44.40	3.00	2.81	93	
	14	44.40	45.40	1.00	0.77	77	
	15	45.40	47.40	2.00	2.64	132	
	16	47.40	50.40	3.00	3.24	108	
	17	50.40	53.40	3.00	1.29	43	
	18	50.40	53.40	3.00	1.75	58	
	19	53.40	56.40	3.00	2.51	84	

Total drilled: 56.40 m; total recovered: 34.90 m; recovery: 61.9%.

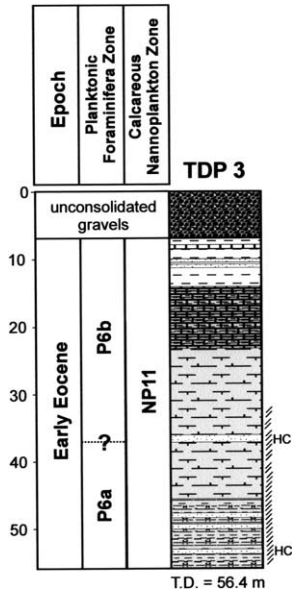

Fig. 9. Integrated litho- and biostratigraphy for TDP Site 3. Symbols are the same as for Fig. 7.

6.2. Lithostratigraphy

Site TDP 3 was spudded-in on soil and unconsolidated coarse gravels, which were discarded. These gravels persist to a depth of 6.9 m. Light olive grey to greyish-olive clays (5Y 5/2 to 10Y 4/2) were cored between 6.9 and 13 m depth. These are mottled and streaked with dark yellowish orange clay. Occasional thin fine quartz sandy clay horizons occur within this interval. There is a sharp change in clay colour and preservation between Cores TDP3/3 and 4, below which an oxidation front is present, in this case being at a depth of between 13.1 and 13.9 m.

Core TDP3/4, from 13.9 to 16.9 m depth, contains a greenish-black to dark greenish grey (5G 2/1 to 5G 4/1) calcareous clay or claystone, verging almost to a marl. This is finely laminated throughout with moderate bioturbation. This lithology persists down to 23.5 m.

From 23.5 to 47.4 m depth, the sediments are dark greenish-grey to greenish-black clay (5G 4/1 to 5G 2/1), with a component of fine to medium carbonate grains dispersed throughout, but concentrating sporadically in horizons with a very fine quartz sand content. Gentle to moderate bioturbation is present throughout the clays which are also finely laminated. Core TDP3/10, at 30.7 m depth, is lithologically identical to those above it but contains inclined laminations from about 15° to 30°. This dip continues for the remainder of the hole which suggests that drilling may have crossed a fault. This does not appear to correspond to any significant age change shown by the microfossil assemblages, however, and may be a minor feature. At 34.4 m depth, the top of a thin carbonate rich, fine quartz sand bed within the clay emitted a pungent smell of oil when first recovered and has a bituminous stain. Organic geochemical analysis (see below) indicates that this is probably migrated oil from outside the formation.

Core TDP3/16, beginning at 47.4 m, marks a change in lithology that extends downward for the remainder of the hole to a final depth of 56.4 m (giving a recovered thickness of 9 m). This lithologically distinct member is composed of a greenish-black (5G 2/1) crumbly and blocky, 'crypto'-laminated, calcareous mudstone to

Table 7
Results of geochemical analyses of samples from TDP Site 3

Sample	Depth (m)	$CaCO_3$ (%)	Sulfur (%)	TOC (%)
TDP 3/2-1, 16-28 cm	10.08–10.20	7.9	0.1	0.2
TDP 3/6-1, 36-45 cm	19.26–19.35	3.7	0.1	0.2
TDP 3/8-1, 48-55 cm	26.88–26.95	1.5	0.2	0.1
TDP 3/12-1, 79-93 cm	37.59–37.73	2.3	0.2	0.4
TDP 3/14-1, 23-29 cm	14.63–14.69	6.0	0.1	0.3
TDP 3/16-2, 73-85 cm*	49.13–49.25	1.5	1.1	0.2
TDP 3/18-1, 74-87 cm	51.14–51.27	4.7	0.2	0.4

Sample highlighted with an asterisk was selected for biomarker study (see Table 1).

claystone. Whereas previously in these cores carbonate cementation in sandier horizons was responsible for the increased lithification of the clays, here there is very little observed carbonate content. A significant mud fraction mixed with the clays seems to have given them a distinct texture and fracture pattern. Thin, fine quartz sand horizons are dispersed within these claystones as before. One of these sands at 60.2 m depth, which is only 2 cm thick, again emitted a bituminous smell on first exposure and is stained. Despite much drilling disturbance at this depth, inclined thin laminations are still visible at sporadic intervals along with mild bioturbation.

The TOC contents of the samples from TDP Site 3 range between 0.1% and 0.4% (Table 7), comparable to TDP Site 2. However, the carbonate and sulfur contents range between 1.5% and 7.9% and 0.1% and 1.1%, respectively, similar ranges as observed for TDP Site 1.

6.3. Planktonic foraminifers

A total of 22 samples from TDP Site 3 were studied for planktonic foraminifers. Preservation of the shells was variable, from excellent in a few samples to poor, especially in the lower part of the well below Core TDP3/14. Samples were oxidized to a depth of about 12.5 m, below which pyrite is abundant and surface oxide staining was not observed. Assemblages are diverse and typically tropical, dominated by morozovellids and acarininids.

Samples down to Sample TDP3/11-1, 14–24 cm were assigned to lower Eocene Zone P6b. Characteristic elements of the assemblages are *Morozovella formosa*, *Morozovella gracilis*, *Morozovella marginodentata*, *Morozovella subbotinae*, and *Igorina lodoensis*. In the absence of *Morozovella aragonensis*, these assemblages were assigned to Subzone P6b. From Sample TDP3/12-1, 72–79 cm to the bottom of the site, no *Morozovella formosa* was observed. *Igorina lodoensis* is also absent below Sample TDP3/12-1, 72–79 cm. The absence of *M. formosa* might indicate that these samples should be assigned to Subzone P6a. However the poor to moderate preservation makes this assignment questionable, as it is based on negative evidence.

6.4. Calcareous nannofossils

Fourteen samples were studied, and yielded moderately-preserved, rare to common nannofossil assemblages, although abundance is generally low in Cores TDP3/14 to TDP3/17. The presence of *Tribrachiatus orthostylus* (NP11-12) (Plate 4(18)), *Zygodiscus herlynii* (NP7-11) (Plate 3(13)) and absence of *Discoaster lodoensis* (marker for NP12), reticulofenestrids (which first occur in mid Zone NP12) and helicosphaerids (first occurrence in basal Zone NP12) indicates a stratigraphic level of Zone NP11, although the topmost sample, which lacks *T. orthostylus*, may lie within lower NP12 (Perch-Nielsen, 1985; Varol, 1989; Bybell and Self-Trail, 1995; Bralower and Mutterlose, 1995). The occurrence of *Sphenolithus conspicuous* (Plate 4(11–12)) in Cores TDP3/1 to TDP3/4 supports a correlation with upper Zone NP11 to NP12 (Bralower and Mutterlose, 1995).

6.5. Benthic foraminifers

Nine samples from TDP Site 3 were studied for benthic foraminifers. Preservations vary from excellent to poor, depending on the extent of carbonate overgrowth and infilling. Species diversity is low for most of the samples. Specimens in cores TDP3/1–TDP3/3 were stained with iron oxide. Benthic foraminifers present include: *Spiroloculina* sp., *Karreriella* sp., *Neoeponides* sp., *Stilostomella* sp., *Pleurostomella* sp., *Fursenkoina* sp., *Heterolepa* sp., *Plectofrondicularia* sp. and *Lenticulina* sp. Unknown species of *Bulimina* and *Praeglobobulimina* were also present throughout the section. Most of the species observed are characteristic of the Eocene. Few samples yield high P:B ratios while others are lower indicating deposition of sediments in marine shelf environment.

6.6. Palynology

Samples from this site are rich in undiagnostic organic particles, which include plant tissues, cuticles and fusinites. However, a few early Eocene dinocyst species were documented, particularly in Sample TDP3/14-1, 37–41 cm, in which dinocysts were abundant, including

Dracodinium condylos and *Cordosphaeridium fibrospinosum*.

6.7. Paleomagnetic analysis

Ten samples were taken for paleomagnetic analysis from relatively undisturbed intervals in TDP Site 3. As at TDP Sites 1 and 2, the resulting data were not considered suitable for magnetostratigraphic interpretation because of probable remagnetization in diagenesis (see Section 3.7 above).

6.8. Organic geochemistry

The saturated hydrocarbon fraction from Sample TDP3/16-2, 15–29 cm has a compound distribution pattern comparable to those observed for TDP Site 1 (Table 1) and is characterized by abundant *n*-alkanes (C_{29} *n*-alkane), hopenes and hopanes and lesser amounts of steranes. As with TDP Site 2, the aromatic hydrocarbon fraction contains neither *n*-alkanones nor PAHs. The TDP Site 3 polar fraction contains the same compound distribution as TDP Site 1 (Table 1). Similar to Sample TDP1/20-2, 14–23 cm, friedelan-3-one (VII; Fig. 4) is the most abundant compound, and similar to TDP 2 the most abundant *n*-alkanol is the C_{30} *n*-alkanol. However, in contrast to TDP Sites 1 and 2, the TDP 3 polar fraction contains neither the C_{15}/C_{15} diether (XI; Fig. 4) nor archeol (XII; Fig. 4).

An additional sample was taken from Sample TDP3/11-1, 65–79 cm, a sandy horizon at which a petroleum-like smell was noted when the core was recovered (see Section 6.1 above). The saturated hydrocarbon fraction has a very different distribution pattern from all other TDP saturated hydrocarbon fractions. It contains a relatively large UCM (unresolved complex mixture; "hump"), typical of heavily biodegraded organic material (including petroleum; Magoon and Claypool, 1985; Gough and Rowland, 1990, 1991; Gough et al., 1992; Revill, 1992; van Dongen et al., 2003). In addition, the hopanes/hopenes and steranes have a thermally mature distribution, characterized by stereoisomers occurring in thermodynamic equilibrium ratios (e.g. ratio of 22S to 22R homohopane is 0.6; Seifert and Moldowan, 1986) rather than dominated by the biological configurations as observed in all other analyzed TDP sediments. The apolar fraction also contains substantial amounts of *n*-alkanes with an odd-over-even predominance similar to but less pronounced than those in other TDP samples. These observations are consistent with the presence of biodegraded petroleum, which on the basis of its anomalously high thermal maturity, must have migrated into the sand horizon from greater depths. The aromatic hydrocarbon and polar fractions contain no detectable higher plant, algal or bacterial biomarkers (neither *n*-alkanols, *n*-alkanoic acids, ω-hydroxy alkanoic acids nor triterpenoids). These lower abundances of in situ (as opposed to petroleum-related) organic matter relative to other sites probably reflect poorer preservation of organic matter either during initial deposition, early diagenesis or later in the sediment history because organic matter in the sandy horizon would have been less protected from bacterial activity and oxidation than organic matter associated with clays. Alternatively, the low abundances of polar biomarker compounds could simply reflect dilution and overprinting by biodegraded petroleum.

6.9. Summary

TDP Site 3 is a relatively short hole varying between greenish-black clays, claystones and muddy claystones. An oxidation front exists at about 13 m core depth. Samples from the un-cemented parts of the site contain well-preserved planktonic microfossils that are suitable for geochemical analysis. The foraminifers (Zone P6) and nannofossils (Zone NP11) both indicate that the sediments are early Eocene in age (about 52.5–53.5 Ma).

Palynological residues and organic geochemistry show that like TDP Sites 1 and 2, there is a large component of terrestrial organic matter such as woody tissue, indicating significant riverine input on to the shelf. Organic geochemical results are similar to those observed at the other sites. However, the sediments at TDP Site 3 contain traces of extra-formational oil in two sandy intervals, the most obvious being in Core TDP3/11. This observation, combined with our previous mapping in the Kilwa area (which resulted in the discovery of a seep at Kilwa Masoko harbour) is of interest regarding hydrocarbon exploration in the area.

Both TDP Sites 2 and 3 cored an interval from lower middle Eocene to the base of the lower Eocene. A considerable break occurs between the holes corresponding to planktonic Zones P8 to P6b. However, clays of the missing zone P7 have previously been sampled in outcrop between the two drill sites at Ras Pungunyuni (UTM 37L 550823, 9019642) during the field survey of 1998. Therefore, although in this paper the drill sites are described separately, in terms of the lithostratigraphy, TDP Sites 2 and 3 should be considered as part of the same formation.

7. TDP Site 4: Ras Tipuli

7.1. Site selection

The Lindi area (Fig. 10) is rich in outcrops of significance in the development of planktonic foraminifer biostratigraphy. Martin, in Blow and Banner (1962) described several samples collected in 1955–1996 from the vicinity of Ras Tapuri (= Tipuli) on the north side of

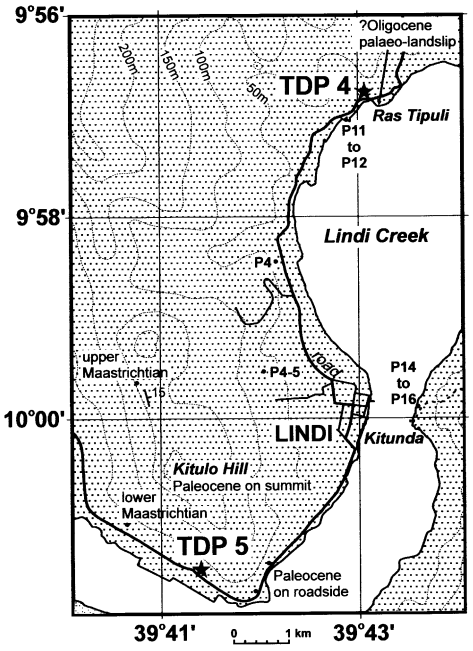

Fig. 10. Location map for TDP Sites 4 and 5 in the Lindi area.

Lindi Bay. One of these (Sample FCRM-1576) was described by Blow and Banner (1962) as the "cotype locality" for their *Globigerina oligocaenica* zone and by Blow (1979) as the "paratype" locality for Zone P19/20 (lower Oligocene). However, no fossil specimens from this sample were illustrated or discussed in the publications by these authors. The holotype of the species *Globigerina tripartita tapuriensis* (Blow and Banner, 1962), despite its name, in fact comes from a sample from Kitunda bluffs on the opposite shore of Lindi Bay. Martin also collected samples from the headland named Ras Umtamar (= Mtama) which is south of Ras Tipuli but these samples were not discussed by Blow and Banner (1962).

North Lindi bay was visited in 1998, 1999 and 2000 and proved to be a very interesting coastal section. The spectacular large scale 'geobreccia' of Neogene limestones at Ras Tipuli was suggested by Kent et al. (1971) to be an ancient collapsed fault scarp related to movement of the nearby Lindi Fault to the east in Lindi Creek. However, a relationship with any supposed 'Lindi fault' cannot be demonstrated and this olistostrome unit is perhaps more likely to be a submarine slump deposit. A number of samples were collected from the small bay to the west of Ras Tipuli including Oligocene sediments in the foreshore containing abundant specimens of the large benthic foraminifer *Lepidocyclina*. The wave-cut platform at Ras Mtama contains an excellent section that has not previously been described but which can be attributed to planktonic foraminifer zones P11 and P12 (middle Eocene).

TDP Site 4 was drilled in a small field adjacent to the Tipuli River about 100 m inland from the bridge west of Ras Tipuli (9°56.999′S, 39°42.985′E). The site was selected because lower Oligocene sediments crop out nearby and according to the map produced by F.C.R. Martin and published by Kent et al. (1971), Oligocene sediments were to be expected there. It was hoped that the site might provide an Eocene–Oligocene boundary section. We were surprised, however, to spud in on middle Eocene sediments. Thus there appears to be a fault passing between TDP-4 and the headland of Ras Tipuli. We had considerable difficulty with core recovery at the site, and technical problems with the water circulation in the rig, so coring was terminated at just 28.2 m. Table 8 shows the depths of cored and drilled intervals and Fig. 11 shows a summary of the litho- and biostratigraphy.

7.2. Lithostratigraphy

After discarding 1 m of topsoil, it was decided to commence coring. However, there was no recovery down to a depth of 8.4 m. This interval contains an extremely friable sandy, white limestone that disintegrated into slurry during drilling. Although a thick Oligocene white limestone is present in the area of the Namadingura River just to the north of Ras Tipuli, it is more likely that the white limestone drilled at the top of TDP Site 4 is Plio-Pleistocene in age, similar to exposures on the coast nearby. It is also interesting to note that the presence of this limestone may have prevented the penetration of modern surface weathering down into

Table 8
Intervals drilled and cored in TDP Site 4 (Ras Tipuli, 9°56.999′S, 39°42.985′E)

Site	Core	Top (m)	Bottom (m)	Drilled (m)	Recovered (m)	Recovery (%)	Comment
TDP4	0	0.00	8.40	8.40	0.00	0	Interval drilled
	1	8.40	11.80	3.40	3.75	110	
	2	11.80	15.30	3.50	0.95	27	Most core lost
	3	15.30	18.50	3.20	1.65	52	
	4	18.50	20.40	1.90	0.61	32	
	5	20.40	23.20	2.80	0.50	18	Most core lost
	6	23.20	26.40	3.20	1.25	39	
	7	26.40	28.20	1.80	0.40	22	

Total drilled: 28.20 m; total recovered: 9.11 m; recovery: 32.3%.

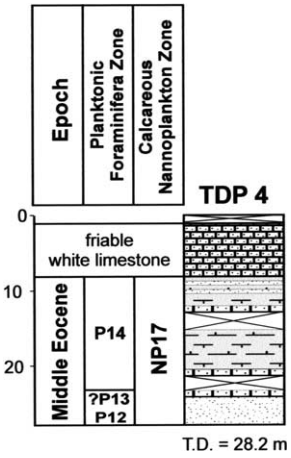

Fig. 11. Integrated litho- and biostratigraphy for TDP Site 4. Symbols are the same as for Fig. 7.

the underlying clays because a deep oxidation front was not observed at this site.

At 8.4 m, coring passed down into dark greenish-grey (5G 4/1) clay with disseminated carbonate grains and a 'sugary' texture, similar to the principal lithology of the Early–Middle Eocene of TDP Sites 2 and 3 in the Kilwa area. Spread throughout this clay are very fine quartz sandy clay horizons in which the carbonate content is higher than the surrounding sediment. A prominent 50 cm thick greenish-grey to light grey (5G 6/1 to N7) benthic foraminifer limestone occurs at 11.8 m. The foraminifers range in size from 0.3 to 2 cm and are crudely normal graded in parts. These features suggest that this limestone bed represents a pulse of benthic foraminifer sand from shallower water. Recovery failed immediately below this bed, but the dark greenish grey sugary clays are present again in the next core at 15.3 m depth. Core recovery remained intermittent until a second, 30 cm thick, benthic foraminifer limestone was encountered at 20.5 m. This is identical in texture and content to the first limestone and the base of this bed marked another loss of core.

At 23.2 m a further 20 cm limestone bed was encountered which contains abundant benthic foraminifers in a medium quartz sand and clay matrix. It also contains some evidence of calcite veining and recrystallization which might suggest either an original hardground developed at this level or that a fault plane may have been present immediately above this bed in the unrecovered interval. Below 23.4 m fine to medium sands are thoroughly mixed with dark greenish-grey clays and drilling mud, destroying any original textures. However, the high sand content in both these mixed clays and also the overlying limestone bed indicates that they should together be identified as a more sandy unit.

The TOC and sulfur contents of the samples from TDP Site 4 range between 0.1% and 0.8% and 0.1% and 0.6%, respectively (Table 9). The carbonate contents range between 4.7% and 13.1%.

7.3. Planktonic foraminifers

A total of eight samples were studied for planktonic foraminifers from TDP Site 4. Preservation is variable, from poor to excellent, and calcite infillings of tests are common. Planktonic foraminifers are generally common and diverse. The presence of *Morozovella spinulosa* and *Hantkenina alabamensis/compressa* in the upper part of the site, as well as *Turborotalia pomeroli*, indicates middle Eocene Zone P14. Sample TDP4/6-1, 44–50 cm contains questionable *Orbulinoides beckmanni* and therefore might be assigned to Zone P13. Sample TDP4/7/CC is below this level and contains *Hantkenina liebsusi* in the absence of *H. alabamensis* and so is assigned to Zone P12.

7.4. Calcareous nannofossils

Five samples were studied, and yielded common to abundant nannofossil assemblages of moderate to good preservation. The assemblages are notably rich in rhabdoliths, holococcoliths, pontosphaerids and pentaliths. The concurrent occurrences of *Helicosphaera compacta* (NP16-24), *Chiasmolithus grandis* (last occurrence in Zone NP17) and *Reticulofenestra* (= *Dictyococcites*) *bisecta* (Plate 3(28)) (first occurrence in Zone NP17) indicates an age of NP17 (Perch-Nielsen, 1985; Varol, 1989; Lyle et al., 2002).

Table 9
Results of geochemical analyses of samples from TDP Site 4

Sample	Depth (m)	$CaCO_3$ (%)	Sulfur (%)	TOC (%)
TDP 4/1-2, 25–38 cm*	9.65–9.78	11.9	0.6	0.4
TDP 4/3-2, 2–12 cm	16.32–16.42	13.1	0.2	0.1
TDP 4/4-1, 31–35 cm	18.81–18.85	4.7	0.1	0.1
TDP 4/5-1, 2–5 cm	20.42–20.45	10.7	0.1	0.2
TDP 4/6-1, 50–60 cm	23.70–23.80	11.5	0.1	0.8

Sample highlighted with an asterisk was selected for biomarker study (see Table 1).

7.5. Benthic foraminifers

Six samples from TDP Site 4 were studied for benthic foraminifers. Species abundance varies, but specimens are present in all the samples except in Sample TDP4/6-1, 40–44 cm. Foraminifer preservation varies from excellent to good. Many new species of small and large benthic foraminifers were observed. Benthic foraminifers present include *Stilostomella nuttalli*, *Stilostomella verneuili*, *Nuttalides truempyi*, and *Anomalinoides alazanensis*, *Planulina renzi*, *Heterolepa* sp., *Asterigerina* sp., *Nummulites* sp., *Lepidocyclina* sp., varieties of *Ammonia*, and *Pararotalia* species (Plate 5(22)). The species *Nuttalides truempyi*, *Anomalinoides alazanensis* and *Planulina renzi* are typical of the middle Eocene. The presence of deep water planktonic and benthic foraminifers together with shallow water large benthonic foraminifers species of *Lepidocyclina*, *Heterostegina*, *Operculina* and *Nummulites* may indicate varying water depths or mixing of sediment on the sea floor.

7.6. Palynology

Six samples were studied. These yielded abundant plant debris and rare dinocysts and miospores. A few diagnostic dinocyst species were documented from the samples. These include *Operculodinium ornamentum* (middle Eocene), *Cordosphaeridium brevispinum* (middle Eocene) and *Homotryblium aculeatum* (Eocene). These occurrences are consistent with the middle Eocene age determination given by foraminifers and nannofossils. The palynology suggests a shelf environment with a relatively high input of terrestrial organic-matter.

7.7. Paleomagnetics

No samples were taken for paleomagnetic analysis from TDP Site 4 because of poor recovery and drilling disturbance.

7.8. Organic geochemistry

The TDP Site 4 saturated hydrocarbon fraction has a compound distribution pattern similar to those observed for TDP Site 1 (Table 1) and is characterized by abundant *n*-alkanes (C_{29} *n*-alkane), hopenes and hopanes and lesser amounts of steranes. As with TDP Site 2, the aromatic hydrocarbon fraction contains neither *n*-alkanones nor PAHs. The TDP Site 4 polar fraction also contains a distribution of compounds similar to that observed in TDP Site 1 (Table 1). However, similar to TDP Site 2, the C_{30} *n*-alkanol is the most abundant *n*-alkanol and similar to TDP Site 3 neither the C_{15}–C_{15}-diether (XI; Fig. 4) nor archeol (XII; Fig. 4) was detected. The TDP Site 4 acid fraction, like those discussed earlier is dominated by *n*-alkanoic acids (Table 1); however, only relatively small amounts of ω-hydroxy alkanoic acids and trace amounts of triterpenoic acids are present. As at the other sites, the organic extracts suggest a high level of terrestrial organic matter input and low thermal maturity.

7.9. Summary

TDP Site 4 contains predominantly dark greenish-grey clay with hard, allochthonous limestone interbeds. The lowermost 5 m of the hole proved to contain abundant sand- and silt-sized quartz grains mixed with the clay, possibly indicating a shallower-water environment than inferred for TDP Sites 2 and 3. Calcareous nannofossils (Zone NP17) and planktonic foraminifers (Zones P12–P14) both suggest a middle Eocene (Bartonian) age (about 39.0–40.5 Ma). Although mostly well preserved, the foraminifers are probably not suitable for geochemical analysis because of frequent calcite infillings of the shells. Palynological preparations indicate a shelf environment with abundant terrestrial organic matter input, presumably from rivers. Organic geochemical results support this interpretation.

There is no known outcrop of precisely this age in the Lindi area, although slightly older sediments (Zones P11–P12) occur at Ras Mtama nearby and slightly younger sediments (Zones P14–P16) are found on the other side of Lindi Bay at Kitunda. The Eocene age of the sediments was unexpected, as Oligocene outcrops are within a few hundred meters of the drill site and the area is marked as lower Oligocene on the geological map prepared by Martin (see Blow and Banner, 1962, Kent et al., 1971). This finding underlines the structural complexity of the area.

8. TDP Site 5: Machole

8.1. Site selection

TDP Site 5 was drilled adjacent to the Lindi to Mtwara Road to the south of Kitulo Hill behind Lindi town (10°01.646′S, 39°41.375′E). The site was selected because Blow (1979) recorded the presence of a lowermost Paleocene outcrop sample here and it was thought possible that a section across the Cretaceous–Tertiary boundary might be obtained. Our previous field surveys had shown that Paleocene limestones and clays were present in situ on the roadside south of Lindi town and that uppermost Maastrichtian clays were exposed on the south-west flank of Kitulo Hill (see Fig. 10). In the event, however, we spudded in on Lower Maastrichtian sediments and so were at a level below the boundary. In retrospect it should be noted that the sediments in this area are greatly confused by slumping off the west side of Kitulo Hill and it is not known if the shallow core

Table 10
Intervals drilled and cored in TDP Site 5 (Machole, 10°01.646′S, 39°41.375′1E)

Site	Core	Top (m)	Bottom (m)	Drilled (m)	Recovered (m)	Recovery (%)	Comment
TDP5	0	0.00	4.00	4.00	0.00	0	Interval drilled
	1	4.00	7.00	3.00	2.52	84	
	2	7.00	11.40	4.40	3.25	74	
	3	11.40	14.40	3.00	1.95	65	
	4	14.40	17.40	3.00	2.16	72	
	5	17.40	20.40	3.00	1.92	64	
	6	20.40	23.40	3.00	3.13	104	
	7	23.40	26.40	3.00	2.88	96	
	8	26.40	27.60	1.20	1.90	158	
	9	27.60	29.40	1.80	3.03	168	
	10	29.40	31.90	2.50	2.95	118	
	11	31.90	32.90	1.00	1.92	192	
	12	32.90	33.60	0.70	0.60	86	
	13	33.60	35.60	2.00	1.70	85	

Total drilled: 35.60 m; total recovered: 29.91 m; recovery: 84.0%.

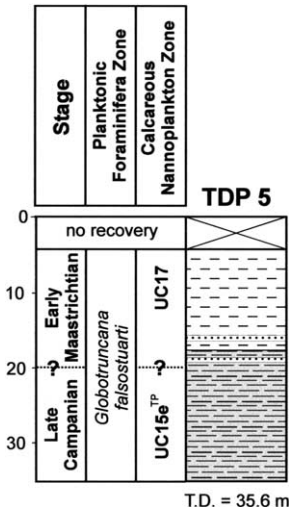

Fig. 12. Integrated litho- and biostratigraphy for TDP Site 5. Symbols are the same as for Fig. 7.

that we drilled was in place or part of a large slump system. Coring was terminated at 35.6 m because we ran out of time for the season's drilling. A list of core depths is presented in Table 10 and a stratigraphic summary is given in Fig. 12.

8.2. Lithostratigraphy

There was no recovery in TDP Site 5 in the top 4 m. From this level, greenish-grey clay was recovered, streaked and mottled with dark yellowish orange clay. The mottling and frequent clay colour changes similar to TDP Sites 1–3 and interpreted as the penetration of modern surface weathering and oxidation, which in this core extends to a depth of 17.4 m. In general, the sediments within this interval are light olive-grey to olive grey (5Y 5/2 to 5Y 3/2) with minor bands of dark greenish-grey to greenish-grey clays (5GY 4/1 to 5G 6/1). All are streaked with light olive-brown to dark yellowish-orange clays (5Y 5/6 to 10YR 6/6). These clays contain dispersed carbonate grains throughout, giving them a 'sugary' texture. At 15.8 m depth, a 25 cm thick orange brown, coarse quartz sandstone was recovered. The grains of this bed are well sorted and sub-rounded, and set in a carbonate cement.

Clays recovered from 17.4 m downwards have a relatively uniform dark greenish-grey colour (5G 4/1), indicating that they are from below the oxidation front. At a depth of 17.9 m a second, thin carbonate cemented coarse quartz sand was cored. Below this sand to the final depth of 35.6 m, the drilling disturbance and mixing with drill mud increased so that no further sedimentary structures are visible.

The TOC, carbonate and sulfur contents of TDP Site 5 sediments range between 0.2% and 0.6%, 5.5% and 9.7% and 0.1% and 0.6%, respectively (Table 11), which is similar to the values obtained from the Paleogene sediments of TDP Sites 1–4.

8.3. Planktonic foraminifers

Planktonic foraminifers from TDP Site 5 are moderately well preserved but are commonly infilled with calcite. The first sediments from Core TDP5/1 yielded species diagnostic of the upper Campanian–lower Maastrichtian *Globotruncana falsostuarti* Zone, indicating that the Danian and upper Maastrichtian sediments identified in the nearby surface samples had been transported from sediment outcrops at a higher level on Kitulo Hill. All subsequent samples to near the bottom of the drill hole (35.3 m depth) were also assigned to the *Globotruncana falsostuarti* Zone.

8.4. Calcareous nannofossils

Twenty-seven samples were analysed for nannofossils through TDP Site 5. Nannofossil preservation is gener-

Table 11
Results of geochemical analyses of samples from TDP Site 5

Sample	Depth (m)	$CaCO_3$ (%)	Sulfur (%)	TOC (%)
TDP 5/2-3, 30–40 cm	9.30–9.40	5.8	0.2	0.4
TDP 5/3-2, 48–57 cm	12.88–12.97	7.7	0.1	0.2
TDP 5/4-2, 74–81 cm	16.14–16.21	8.9	0.2	0.3
TDP 5/5-1, 53–59 cm	17.93–17.99	8.2	0.2	0.3
TDP 5/7-1, 20–32 cm	23.60–23.73	8.6	0.2	0.4
TDP 5/8-1, 91–104 cm	27.31–27.44	9.3	0.2	0.4
TDP 5/9-3, 33–45 cm*	29.93–30.05	9.7	0.6	0.4
TDP 5/11-2, 65–81 cm	33.55–33.71	5.5	0.3	0.6
TDP 5/13-1, 12–22 cm	33.72–33.82	6.3	0.2	0.4

Sample highlighted with an asterisk was selected for biomarker study (see Table 1).

ally moderate to good throughout. The presence of *Uniplanarius trifidus* and *Tramolithus orionatus* (along with *Reinhardtites levis*) in the topmost sample, Sample TDP5/1-1, 60–61 cm, indicates UC17 at the top, equivalent to an age of early Maastrichtian. The last occurrence of *Broinsonia parca constricta* at Sample TDP5/2-2, 79–80 cm indicates proximity to the Campanian/Maastrichtian boundary. Burnett (1998) placed the boundary within UC17 (between the LO of *B. parca constricta* and the LO of *Tranolithus orionatus*), however, Gardin et al. (2001) redetermined this boundary as being older, lying between the last occurrences of *Eiffellithus eximius* and *B. parca constricta* (i.e. in UC16). Consequently the Campanian/Maastrichtian boundary lies somewhere between Sample TDP5/6-1, 70–71 cm and TDP5/2-2, 79–80 cm.

The basal sample (Sample TDP5/12-1, 22–23 cm) contains *Eiffellithus parallelus* and *U. trifidus*, thus falls into Subzone UC15e^{TP}, indicating a late Campanian age. This zone is further supported at Sample TDP5/6-3, 36–37 cm by the first occurrence (FO) of *Cylindralithus*? *nieliae* and also possibly at Sample TDP5/6-2, 48–49 cm by the probable last occurrence of curved spines (although there is a single occurrence of a curved spine in Sample TDP5/1-1, 60–61 cm, which is herein interpreted as having been reworked). The marker-event for the base of Zone UC16 (last occurrence of *E. eximius*) is not identifiable in this succession, the marker being absent. (n.b. Lees, 2002, noted this taxon's similarly enigmatic absence from ODP Hole 758A, northern end of the Ninetyeast Ridge, Bay of Bengal.)

New species of *Corollithion*, *Eiffellithus*, *Micula*, *Staurolithites* and *Zeugrhabdotus*, along with some holococcolith taxa, were identified. These will be described elsewhere.

According to Lees (2002), Tanzania was situated in the Tropical Nannofossil Paleobiogeographical Zone (PBZ) in the Late Campanian. A lack of data for the low-latitude Indian Ocean early Maastrichtian meant that she could not identify the southern boundary of the Tropical PBZ for that interval. Consequently, the Tanzanian nannofloras constitute a vital part of the nannofossil biogeography for the region.

8.5. Benthic foraminifers

Benthic forminifer assemblages reveal a predominance of agglutinated and nodosariid species with P:B ratios typically 40–60%. Preservation varies markedly from sample to sample, from Good to Poor. Common genera include *Bolivina*, *Gavelinella*, *Angulogavalinella*, *Praebulimina*, *Dorotia*, *Lenticulina*, *Neoflabellina*, *Osangularia*, *Anomalinoides*, and *Quinquiloculina*.

8.6. Palynology

Fourteen samples were studied for palynology from this site. Cavate/proximate dinoflagellate cysts are common, while miospores are generally rare. Samples yielded typical Campanian–Maastrichtian dinocyst species. The significant diagnostic taxa documented from the samples, and their age-ranges from the literature, include *Trichodinium bifurcatum* (Maastrichtian), *Andalusiella mauthei* (Senonian) (Plate 6(18)), *Senegalinum bicavatum* (Campanian–Maastrichtian) (Plate 6(17)), *Dinogymnium westralium* (Senonian), *Trichodinium castanea* (Senonian) and *Palaeohystrichophora infusorioides* (Senonian). Others include *Dinogymnium digitus* (Senonian), *Alisogymnium downiei* (Campanian–Maastrichtian) (Plate 6(12)), *Dinogymnium acuminatum* (Maastrichtian) (Plate 6(15)), *Prolixosphaeridium granulosum* (Senonian), *Dinogymnium pustulicostatum* (Campanian–Maastrichtian), *Dinogymnium longicorne* (Senonian), *Hapsocysta peridictya* (Aptian-Late Cretaceous), *Pervosphaeridium pseudohystrichodinium* (Late Cretaceous) and *Callaiosphaeridium asymmetricum* (Senonian).

The Maastrichtian for TDP Site 5 is marked by the presence of *Cordosphaeridium* spp., *Paleocystodinium* spp., *Areoligera* spp. and *Ceratiopsis* spp. in Sample TDP5/3-1, 45–49 cm (Plate 6(11) and (13)). *Areoligera* spp. and *Ceratiopsis* spp. range from Upper Campanian to Maastrichtian (Powell, 1992). The dinocyst species *Cerodinium diebelii* (stratigraphic range, uppermost Maasrichtian–earliest Paleocene, according to Powell, 1992, and Senonian–Paleocene according to Lentin and

Williams, 1993) is very common across the Cretaceous/Tertiary boundary (Powell, 1992). *C. diebelii* was common in the studied samples.

Typical lower Maastrichtian forms, which include *Odontochitina* were rare. Only one specimen was recorded from Sample TDP5/11-2, 51–56 cm. Typical upper Campanian species which include *Trichodinium* spp. (top range: Campanian) (Plate 6(20)), *Areoligera* spp. (top range: Uppermost Campanian), *Callaiosphaeridium asymmetricum* (top range: upper Campanian) (Plate 6(21)) and *Palaeohystichophora infusoriodes* (top range, upper Campanian) (Powell, 1992) were recorded from the samples. Typical Lower Campanian species, which include *Isabelidinium* spp. and *Chatangiella* spp., were very rare. Only one poorly preserved specimen of *Chatangiella* was recorded from Sample TDP5/13-1, 33–40 cm and this may have been reworked.

8.7. Paleomagnetic analysis

As discussed in Section 3.7, TDP Site 5 is the only drill-site for which paleomagnetic data can be clearly interpreted in a way that is consistent with biostratigraphic constraints. It is possible that the magnetic polarity data from TDP Site 5 may not be reliable, for similar reasons as TDP Sites 1, 2 and 3. However, the different demagnetization characteristics for samples from TDP Site 5 (Fig. 13) indicate a different magnetic mineralogy for this hole. The presence of magnetic iron sulfides is not clearly evident in these data. Detailed rock magnetic results, and SEM observations of polished sections, would be required to demonstrate a difference in magnetic mineralogy at TDP Site 5 compared to the other holes. Such data are currently not available. We therefore interpret the magnetostratigraphy of TDP Site 5 under the assumption that the paleomagnetic record is indicative of a syn-depositional magnetization that provides constraints on the geochronology.

Planktonic foraminifers, calcareous nannofossils and dinocysts indicate that sediments recovered in TDP Site 5 are of early Maastrichtian and late Campanian age. The magnetic polarity stratigraphy consists of a thin upper normal polarity zone at the top of the sampled interval, which is underlain by a thin reversed polarity zone and then by a thick normal polarity zone (Fig. 14). The paleomagnetic inclinations are variable, but generally have values of ±20–40°. The apparent polar-wander path of Besse and Courtillot (2002) indicates that the African Plate would have been about 15° further south during the Maastrichtian and upper Campanian. This suggests a paleolatitude of 25° S for the drill-site, which gives an expected inclination of ±43°. This expected value is a little steeper than observed in TDP Site 5. Compaction-related shallowing of

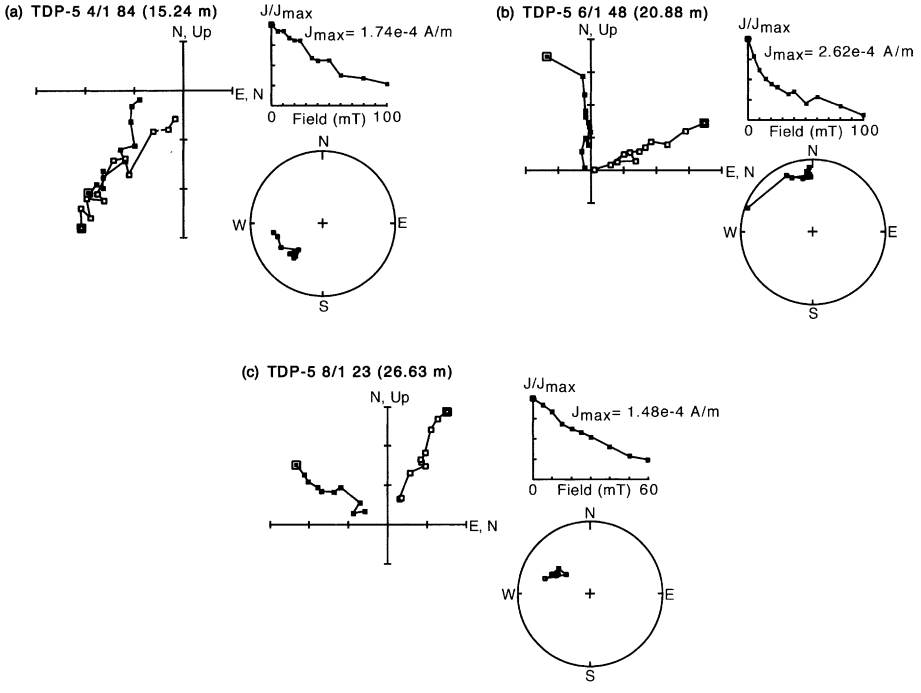

Fig. 13. Representative vector component diagrams for samples from TDP Site 5. Samples from 15.24 m (reversed polarity), 20.88 m (normal polarity) and 26.63 m (normal polarity), while relatively weakly magnetized, with slightly noisy demagnetization trajectories, have clearly-defined characteristic remanent magnetization directions. Projections onto the vertical (horizontal) plane are represented by open (solid) symbols, respectively. Sub-plots indicate decay of magnetization during demagnetization treatment (upper) and the variation of the direction of magnetization during demagnetization treatment (lower), which is plotted on an equal-area stereographic projection. Open (solid) symbols denote projections onto the upper (lower) hemisphere.

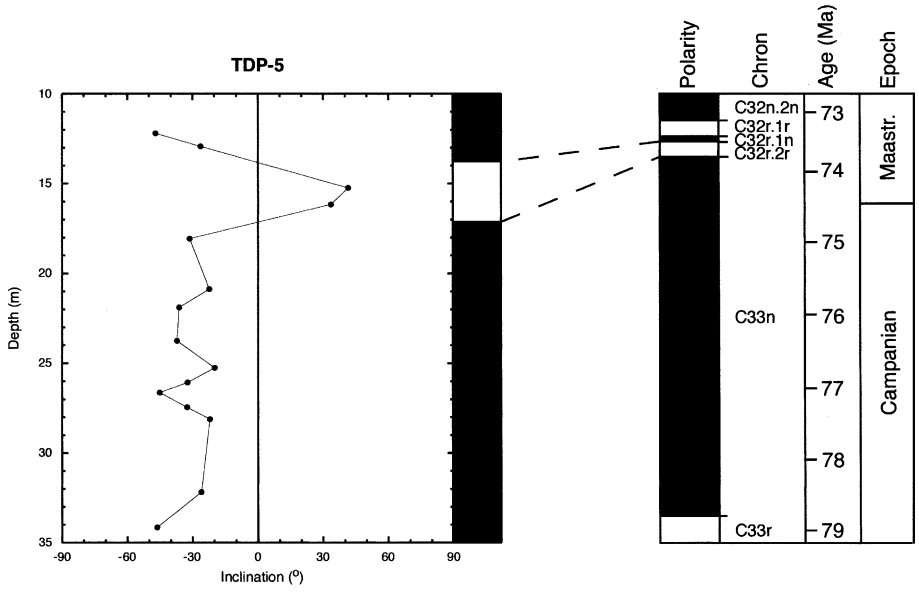

Fig. 14. Down-core variations of paleomagnetic inclinations from TDP Site 5, with the magnetic polarity stratigraphy derived from the inclination data (black (white) = normal (reversed) polarity). Correlation to the geomagnetic polarity timescale of Cande and Kent (1995) is shown on the right.

paleomagnetic inclinations is commonly observed in clastic sedimentary rocks (Anson and Kodama, 1987), which might be responsible for the observed shallow inclinations.

Planktonic foraminifers and calcareous nannofossils indicate that the upper Campanian to lower Maastrictian boundary occurs in the lower part of TDP Site 5. This boundary occurs within a >5 Myr. interval of normal polarity (Chron C33n). It therefore seems likely that the lower normal polarity zone in TDP Site 5 correlates with Chron C33n. The reversed and normal polarity zones in the upper part of TDP Site 5 probably correlate with the immediately overlying Lower Maastrictian polarity chrons C32r.2r and C32r.1n, respectively. If this correlation is correct, it places age-limits on the two polarity transitions at ~17 and ~14 m, respectively (73.62 and 73.37 Ma, respectively). The long duration of Chron C33n (79.08–73.62 Ma) and the fact that it is not observed in its entirety in TDP Site 5 makes it impossible to place tighter paleomagnetic constraints on the age of the lower part of TDP Site 5.

8.8. Organic geochemistry

The TDP Site 5 saturated hydrocarbon fraction has a compound distribution pattern comparable to those observed of TDP Site 1 (Table 1) and is characterized by abundant *n*-alkanes (C_{31} *n*-alkane), hopenes and hopanes and lesser amounts of steranes. As with TDP Site 2, the aromatic hydrocarbon fraction contains neither *n*-alkanones nor PAHs. The TDP Site 5 polar fraction contains a similar compound distribution as TDP Site 1 (Table 1), with the C_{28} *n*-alkanol as the most abundant *n*-alkanol. However, as in TDP Sites 3 and 4, neither the C_{15}–C_{15}-diether (XI; Fig. 4) nor archeol (XII; Fig. 4) was detected. The distribution pattern in the TDP Site 4 acid fraction is comparable to TDP Site 1 (Table 1), although no triterpenoic acids were detected. In addition, the C_{22} ω-hydroxy alkanoic acid is the most abundant compound present, comparable to Sample TDP1/11-1, 39–50 cm, and trace amounts of α-hydroxy alkanoic acids are present. These results indicate a high concentration of terrestrial organic matter and very low thermal maturity as at the other sites drilled.

8.9. Summary

The dominant lithology throughout TDP Site 5 is a dark green to brown mudstone. Preservation of foraminifers varies from poor to moderate, with many specimens infilled by pyrite or calcite. Foraminifers are common to abundant in all samples and planktonic abundances range between 40% and 50%. This, combined with the abundance of agglutinated and nodosariid benthic foraminifers, suggests that the cored sequence was deposited in an outer shelf environment in relatively deep water. The dinocyst evidence also supports this interpretation.

Nannofossils (Zones UC15–UC17), foraminifers (*Globotruncana falsostuarti* Zone) and palynomorphs all suggest that the site crosses the Campanian–Maastrichtian boundary interval (about 72 Ma). This site was the only one in which potentially useful magnetostratigraphic data were obtained, indicating that TDP Site 5 straddles two magnetic reversals between Chrons C322.2r and C32r.1n.

9. Conclusions

The Tanzania Drilling Project cored five sites in 2002, yielding sediments ranging in age from Upper Cretaceous (Campanian) to Oligocene. All of the sites are dominated by clays and many samples contain excellently preserved microfossils that are suitable for a wide range of geochemical analyses. The cores were dated by a combination of planktonic foraminifer and calcareous nannofossil biostratigraphies with additional information from benthic foraminifers and palynomorphs. In one site (TDP Site 5), the paleomagnetic data was also considered suitable for magnetostratigraphic interpretation.

Ratios of planktonic to benthic foraminifers and the benthic assemblages can be used to suggest approximate water-depths for the various samples obtained. The Oligocene sediments obtained in TDP Site 1 are interpreted as having been deposited in a relatively shallow, anoxic, possibly estuarine or deltaic, setting. The Eocene and Cretaceous sediments in TDP Sites 2, 3, 4 and 5 are all interpreted as having been deposited in an open shelf environment with substantial water depths, although minor differences in relative sea-level may be responsible for variations in P:B ratios, benthic foraminifer and dinocyst assemblages. Beds of allochthonous shallow-water sediment (such as larger benthic foraminifer shells and sand) are present as a minor component in all sites. Clay analysis suggests that much of the clay in the Paleogene may have been derived from exposed Mesozoic clays.

Organic geochemical analyses of samples from each of the cores reveals biomarkers of predominantly terrestrial origin. Also present are substantial abundances of bacterial derived hopanoids; further evidence for microbial contributions come from the presence of the C_{15}/C_{15} diether and archaeol in TDP Sites 1 and 2; as these compounds are relatively labile, they were possibly present at one time in the older sediments at other sites 3–5. These organic-matter assemblages clearly indicate a continental shelf setting dominated by higher plant inputs, probably related to fluvial processes. The delivery of high amounts of terrestrial organic matter probably stimulated sedimentary microbial activity, including sulfate reduction. Biomarker evidence for marine productivity is limited to the steroids; in particular, the presence of 4,24-dimethylcholestan-3-one and other 4-methylsteroids is probably indicative of a dinoflagellate input, consistent with palynological analyses. In one case (TDP Site 3) traces of migrated oil were discovered.

The total drilled in 2002 represents only about 12% of the total thickness of the Paleogene beds suggested by R. Stonely on the basis of surveys conducted in the 1950s (see Kent et al., 1971). That figure may represent an overestimate, however, because changes in dip and repetitions by unobserved faults may have produced broader outcrop traces than would occur in the case of simple layer-cake stratigraphy. Further drilling may help reveal the true thicknesses of the units and the extent of so-far unrecovered strata.

The results presented here are the first detailed integrated stratigraphic investigations to be conducted on the Paleogene and upper Cretaceous sediments of the area. The sediments of the East African margin hold great promise in the fields of tropical paleoceanography and paleoclimate research. Further drilling in Tanzania, and indeed along the whole margin, is likely to be of great interest in providing windows into ancient marine environments with well-preserved microfossils.

Acknowledgements

We are grateful to the Natural Environment Research Council for providing funds for this drilling research, the Tanzania Petroleum Development Corporation for extensive logistical and scientific support, and to the Tanzania Commission for Science and Technology (COSTECH) for permission to drill. The manuscript benefited from reviews by Isabella Raffi and one anonymous reviewer. We thank the District Commissioner, District Administrative Officer and the District Executive Director in Kilwa, and the Regional Administrative Officer and District Administrative Officer in Lindi for facilitating our research and making us welcome. Ephrem Mchana and Michael Mkereme provided expert technical assistance during drilling operations. Finally we are grateful to Elvis Mgaya ('Mr. K') for driving while maintaining a sharp eye for clay outcrop.

References

Ahmad, M., Neale, J.W., Siddiqui, Q.A., 1991. Tertiary Ostracoda from the Lindi area, Tanzania. Bull. Br. Mus. Nat. Hist. (Geol.) 46, 175–270.

Anson, G.L., Kodama, K.P., 1987. Compaction-induced shallowing of the post-depositional remanent magnetization in a synthetic sediment. Geophys. J. R. Astron. Soc. 88, 673–692.

Aubry, M.-P., 1983. Biostratigraphie du Paléogène épicontinental de l'Europe du Nord-Ouest. Étude Fondée sur les Nannofossiles Calcaires. Documents des laboratoires de géologie Lyon 89, 1–317.

Aubry, M.-P., 1991. Sequence stratigraphy: eustacy or tectonic Imprint? J. Geophys. Res. 96, 6641–6679.

Aubry, M.-P., 1999. Book 5: Heliolithae (Zygoliths and Rhabdoliths). In: Handbook of Cenozoic Calcareous Nannoplankton. Micropaleontology Press, American Museum of Natural History, New York.

Barss, M.S., Williams, G.L., 1973. Palynology and nannofossil processing techniques. Geological Survey Canada, Paper 73–26, 25 pp.

Bate, R.H., Bayliss, D.D., 1969. An outline account of the Cretaceous and Teriary Foraminifera and of the Cretaceous ostracods of Tanzania. In: Proceedings of the 3rd African Micropaleontologic,

Colloq., 113–164. Nat. Inform. Document Centre, Centre (NIDOC), Cairo.

Berggren, W.A., Kent, D.V., Swisher, C.C., Aubry, M.-P., 1995. A revised Cenozoic geochronology and chronostratigraphy. In: Berggren, W.A., Kent, D.V., Aubry, M.P., Hardenbol, J. (Eds.), Geocheonology, Time Scales and Global Stratigraphic Correlation. In: SEPM Spec. Publ., No. 54, pp. 129–212.

Besse, J., Courtillot, V., 2002. Apparent and true polar wander and the geometry of the geomagnetic field over the last 200 Myr. J. Geophys. Res., 107. doi: 10.1029/2000JB000050.

Blow, W.H., 1979. The Cainozoic Globigerinida: A Study of the Morphology, Taxonomy and Evolutionary Relationships and the Stratigraphical Distribution of Some Globigerinida (mainly Globigerinacea). 3 vols. E.J. Brill, Leiden, 1308 pp.

Blow, W.H., Banner, F.T., 1962. The Mid-Tertiary (Upper Eocene to Aquitanian) Globigerinacea. In: Eames, F.T. et al. (Eds.), Fundamentals of mid-Tertiary Stratigraphic Correlation. Cambridge University Press, London, pp. 61–151.

Bown, P.R., Young, J.R., 1998. Techniques. In: Bown, P.R. (Ed.), Calcareous Nannofossil Biostratigraphy. Kluwer Academic, pp. 16–28.

Bralower, T.J., Mutterlose, J., 1995. Calcareous nannofossil biostratigraphy of Site 865, Allison Guyot, Central Pacific Ocean: a tropical Paleogene reference section. In: Proceedings of the ODP, Scientific Results 143, pp. 31–74.

Burnett, J.A. (with contributions from Gallagher, L.T. and Hampton, M.J.), 1998. Upper Cretaceous. In: Bown, P.R. (Ed.), Calcareous Nannofossil Biostratigraphy. British Micropaleontological Society Series. Chapman & Hall, Kluwer Academic Press, pp. 132–199.

Bybell, L.M., Self-Trail, J.M., 1995. Evolutionary, biostratigraphic, and taxonomic study of calcareous nannofossils from the continuous Paleocene–Eocene boundary section in New Jersey. US Geological Survey Professional Paper 1554, 36 pp.

Cande, S.C., Kent, D.V., 1995. Revised calibration of the geomagnetic polarity time scale for the late Cretaceous and Cenozoic. J. Geophys. Res. 100, 6093–6095.

Coxall, H.K., Huber, B.T., Pearson, P.N., 2003. Origin and morphology of the Eocene planktonic foraminifer *Hantkenina*. J. Foraminiferal Res. 33, 237–261.

de Kaenel, E., Villa, G., 1996. Oligocene–Miocene calcareous nannofossil biostratigraphy and paleoecology from the Iberia Abyssal Plain. Proc. ODP, Sci. Res. 149, 79–145.

Eglinton, G., Hamilton, R.J., 1963. The distribution of *n*-alkanes. In: Swain, T. (Ed.), Chemical Plant Taxonomy. Academic Press, pp. 187–217.

Eglinton, G., Hamilton, R.J., 1967. Leaf epicuticular waxes. Science 156, 1322–1335.

Ernst, G., Zander, J., 1993. Stratigraphy, facies development, and trace fossils of the Upper Cretaceous of southern Tanzania (Kilwa District). In: Geology and Mineral resources of Somalia and surrounding areas, Inst. Agron. Oltremare Firenze, Relaz. E Monogr. 113, Firenze, pp. 259–278.

Fahrion, H., 1937. Die Foraminiferen der Kreide- und Tertiär-Schichten im südlichen Deutsch-Ostafrika. Palaeontographica Suppl. VII, Zweite Reihe, II, Stuttgart, pp. 187–216.

Florindo, F., Sagnotti, L., 1995. Paleomagnetism and rock magnetism in the upper Pliocene Valle Ricca (Rome, Italy) section. Geophys. J. Int. 123, 340–354.

Gardin, S., Odin, G.S., Bonnemaison, M., Melinte, M., Monechi, S., von Salis, K., 2001. Results of the cooperative study on the calcareous nannofossils across the Campanian–Maastrichtian boundary at Tercis les Bains (Landes, France). In: Odin, G.S. (Ed.), The Campanian–Maastrichtian Stage Boundary. Characterisation at Tercis les Bains (France) and Correlation with Europe and other Continents. In: Developments in Paleontology and Stratigraphy, vol. 19. Elsevier, Amsterdam, pp. 293–309.

Gierlowski-Kordesch, E., Ernst, G., 1987. A flysch trace assemblage from the Upper Cretaceous shelf of Tanzania. In: Matheis, G., Schandelmeier, H. (Eds.), Current Res. African Earth Sci.. Rotterdam, pp. 217–222.

Gough, M.A., Rowland, S.J., 1990. Characterization of unresolved complex mixtures of hydrocarbons in petroleum. Nature 344, 759–761.

Gough, M.A., Rowland, S.J., 1991. Characterization of unresolved complex mixtures of hydrocarbons from lubricating oil feedstocks. Energy Fuels 5, 648–650.

Gough, M.A., Rhead, M.M., Rowland, S.J., 1992. Biodegradation studies of unresolved complex mixtures of hydrocarbons: model UCM hydrocarbons and the aliphatic UCM. Org. Geochem. 18, 17–22.

Gradstein, F.M., Agterberg, F.P., Ogg, J.G., Hardenbol, J., van Veen, P., Thierry, J., Huang, Z., 1995. A Triassic, Jurassic and Cretaceous time scale. In: Berggren, W.A., Kent, D.V., Aubry, M.P., Hardenbol, J. (Eds.), Geocheonology, Time Scales and Global Stratigraphic Correlation. In: SEPM Spec. Publ., No. 54, pp. 95–126.

Haughton, S.H. (Ed.), 1938. Africa. In: Lexicon de Stratigraphie, vol. 1. Thomas Murby, London. 432 pp.

Hennig, E., 1937. Der Sedimentstreifen des Lindi–Kilwa-Hinterlandes. Palaeontographica, Suppl. VII, Zweite Reihe, II, pp. 99–186, 13–15.

Holloway, P.J., 1982. The chemical constitution of plant cutins. In: Cutler, D.F., Alvin, K.T., Price, C.E. (Eds.), The Plant Cuticle. Linnean Soc. Lond. Academic Press, London, pp. 45–85.

Horng, C.-S., Torii, M., Shea, K.-S., Kao, S.-J., 1998. Inconsistent magnetic polarities between greigite- and pyrrhotite/magnetite-bearing marine sediments from the Tsailiao-chi section, southwestern Taiwan. Earth Planet Sci. Lett. 164, 467–481.

Jiang, W.T., Horng, C.S., Roberts, A.P., Peacor, D.R., 2001. Contradictory magnetic polarities in sediments and variable timing of neoformation of authigenic greigite. Earth Planet Sci. Lett. 193, 1–12.

Kates, M., Kushner, D.J., Matheson, A.T., 1993. The Biochemistry of Archaea (Archaebacteria). Elsevier, Amsterdam. 582 pp.

Kent, P.E., Hunt, J.A., Johnstone, D.W., 1971. The Geology and Geophysics of Coastal Tanzania. Institute of Geological Sciences Geophysical Paper No. 6, i–vi, 1–101. HMSO, London.

Kim, H.Y., Salem Jr., N., 1990. Separation of lipid classes by solid phase extraction. J. Lipid Res. 31, 2285–2289.

Kirschvink, J.L., 1980. The least-squares line and plane and the analysis of paleomagnetic data. Geophys. J. R. Astron. Soc. 62, 699–718.

Koga, Y., Morii, H., Akagawa-Matsushita, M., Ohga, M., 1993. Ether lipids of methanogenic bacteria: structures, comparative aspects, and biosyntheses. Microbiol. Res. 57, 164–182.

Lawver, L.A., Coffin, M.F., Falvey, D.A., 1992. The Mesozoic breakup of Gondwana. In: First Indian Ocean Petroleum Seminar, pp. 345–356.

Lees, J.A., 2002. Calcareous nannofossil biogeography illustrates paleoclimate change in the Late Cretaceous Indian Ocean. Cretaceous Res. 23, 537–634.

Leif, R.N., Simoneit, B.R.T., 1995. Ketones in hydrothermal petroleums and sediment extracts from Guaymas Basin, Gulf of California. Org. Geochem. 23, 889–904.

Lentin, J.K., Williams, G.L., 1993. Fossil dinoflagellates, index to genera and species, 1993 edition. Contribution series No. 28. American Association of stratigraphic palynologists, pp. 1–856.

Lyle, M.W., Wilson, P.A., Janacek, T.R., et al., 2002. Proc. ODP, Init. Repts., 199 [CD ROM].

Magoon, L.B., Claypool, C.E., 1985. Alaska North slope oil rock correlation study. The American Association of Petroleum Geologists, Tulsa.

Martini, E., 1971. Standard Tertiary and Quaternary calcareous nannoplankton zonation. In: Faranacci (Ed.), Proceedings of the

Second Planktonic Conference Roma 1970, Edizioni Tecnoscienza, Rome, vol. 2, pp. 739–785.

Moore, W.R., McBeath, D.M., Linton, R.E., Terris, A.P., Stoneley, R., 1963. Geological Survey of Tanganyika Quarter Degree Sheet 256 & 256E. 1:125 000. Kilwa. First ed. Geological Survey Division, Dodoma.

Norris, R.D., Wilson, P.A., 1998. Low-latitude sea-surface temperatures for the mid-Cretaceous and the evolution of planktic foraminifera. Geology 26, 823–826.

Norris, R.D., Bice, K.L., Magno, E.A., Wilson, P.A., 2002. Jiggling the tropical thermostat in the Cretaceous hothouse. Geology 30, 299–302.

Okada, H., Bukry, D., 1980. Supplementary modification and introduction of code numbers to the low-latitude coccolith biostratigraphic zonation (Bukry, 1973; 1975). Marine Micropaleontol. 5, 321–325.

Ourisson, O., Albrecht, P., Rohmer, M., 1979. The hopanoids. Pure Appl. Chem. 51, 709–729.

Pancost, R.D., Boulaoubassi, I., Aloisi, G., Sinninghe Damsté, J.S., Medinaut Shipboard Scientific Party, 2001. Three series of non-isoprenoidal dialkyl glycerol diethers in cold-seep carbonate crusts. Org. Geochem. 32, 695–707.

Pearson, P.N., Ditchfield, P.W., Singano, J., Harcourt-Brown, K.G., Nicholas, C.J., Olsson, R.K., Shackleton, N.J., Hall, M.A., 2001. Warm tropical sea surface temperatures in the Late Cretaceous and Eocene epochs. Nature 413, 481–487.

Pearson, P.N., Ditchfield, P.W., Shackleton, N.J., 2002. Paleoclimatology (communication arising): tropical temperatures in greenhouse episodes. Nature 419, 898.

Perch-Nielsen, K., 1985. Mesozoic calcareous nannofossils. In: Bolli, H.M., Saunders, J.B., Perch-Nielsen, K. (Eds.), Plankton Stratigraphy. Cambridge University Press, Cambridge, pp. 329–426.

Powell, A.J. (Ed.), 1992. A Stratigraphic Index of Dinoflagellate Cysts. British Micropaleontology Society Publication Series, 290 pp.

Ramsay, W.R., 1962. Hantkenininae in the Tertiary rocks of Tanganyika. Cont. Cushman Found. Foram. Res. 13, 78–89.

Revill, A.T., 1992. Use of oxidative degradation followed by capillary gas chromatography-mass spectrometry and multidimensional scaling analysis to fingerprint unresolved complex mixtures of hydrocarbons. J. Chrom. 589, 281–286.

Roberts, A.P., 1995. Magnetic characteristics of sedimentary greigite (Fe_3S_4) Earth Planet. Sci. Lett. 134, 227–236.

Sagnotti, L., Winkler, A., 1999. Rock magnetism and paleomagnetism of greigite-bearing mudstones in the Italian peninsula. Earth Planet Sci. Lett. 165, 67–90.

Salman, G., Abdula, I., 1995. Development of the Mozambique and Ruvuma sedimentary basins, offshore Mozambique. Sed. Geol. 96, 7–41.

Schlüter, T., 1997. Geology of East Africa. Borntraeger, Stuttgart. 512 pp.

Seifert, W.K., Moldowan, J.M., 1986. Use of biological markers in petroleum exploration. In: Johns, R.B. (Ed.), Methods in Geochemistry and Geophysics, vol. 24, pp. 261–290.

Simiyu, S.M., Keller, G.R., 1997. An integrated analysis of lithospheric structure across the East African plateau based on gravity anomalies and recent seismic studies. Tectonophysics 278, 291–313.

Sissingh, W., 1977. Biostratigraphy of Cretaceous calcareous nannoplankton. Geol. Mijnbouw 56, 37–65.

van Dongen, B.E., Schouten, S., Sinninghe Damsté, J.S., 2003. Sulfurization of carbohydrates results in a S-rich, unresolved complex mixture in kerogen pyrolysates. Energy Fuels 17, 1109–1118.

Varol, O., 1989. Eocene calcareous nannofossils from Sile (northwest Turkey). Revista Española de Micropaleontologîa 21, 273–320.

Volkman, J.K., Kearney, P., Jeffrey, S.W., 1990. A new source of 4-methyl sterols and 5a(H)-stanols in sediments: prymnesiophyte microalgea of the genus *Pavlova*. Org. Geochem. 15, 489–497.

Volkman, J.K., Barrett, S.M., Dunstan, G.A., Jeffrey, S.W., 1993. Geochemical significance of the occurrence of dinosterol and other 4-methyl sterols in a marine diatom. Org. Geochem. 20, 7–15.

Volkman, J.K., Rijpstra, W.I.C., de Leeuw, J.W., Mansour, M.P., Jackson, A.E., Blackburn, S.I., 1999. Sterols of four dinoflagellates from the genus *Prorocentrum*. Phytochemistry 52, 659–668.

Weaver, R., Roberts, A.P., Barker, A.J., 2002. A late diagenetic (synfolding) magnetization carried by pyrrhotite: implications for paleomagnetic studies from magnetic iron sulphide-bearing sediments. Earth Planet Sci. Lett. 200, 371–386.

Wilson, P.A., Norris, R.D., 2001. Warm tropical ocean surface and global anoxia during the mid-Cretaceous period. Nature 412, 425–429.

Wilson, P.A., Norris, R.D., Cooper, M.J., 2002. Testing the Cretaceous greenhouse hypothesis using glassy foraminiferal calcite from the core of the Turonian tropics on Demerara Rise. Geology 30, 607–610.

Withers, N.W., Tuttle, R.C., Holz, G.G., Beach, D.H., Goad, L.J., Goodwin, T.W., 1978. Dehydrodinosterol, dinosterone and related sterols of a non-photosynthetic dinoflagellate, *Crypthecodinium cohnii*. Phytochem. 17, 1987–1989.